

Astro/Phys 224

Spring 2014

Origin and Evolution of the Universe

Week 5

Structure Formation

Joel Primack

University of California, Santa Cruz

Physics 224 - Spring 2014 – Tentative Term Project Topics

Adam Coogan – The BICEP2 Result and Its Implications for Inflationary Cosmology

Devon Hollowood – Some Aspect of the Dark Energy Survey

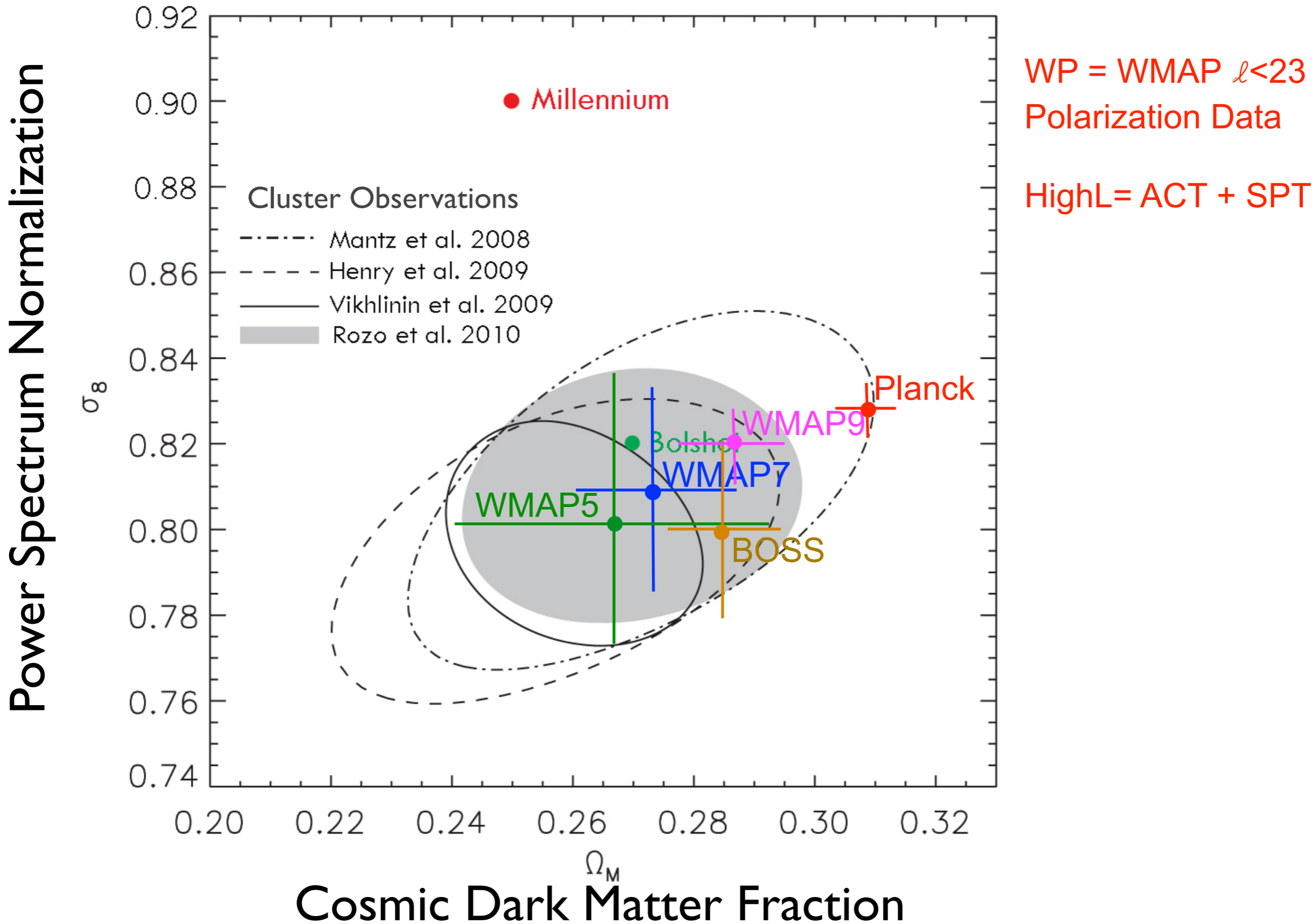
Caitlin Johnson – Observing Plan for ACTs to Constrain the Long-Wavelength EBL

Thomas Kelly – Various Methods of Testing Modified Newtonian Dynamics (MOND)

Tanmai Sai – Shapes of Simulated Galaxies

Vivian Tang – Studying Galaxy Evolution by Comparing Simulations and Observations

Determination of σ_8 and Ω_M from CMB+ WMAP9+SN+Clusters Planck+WP+HighL+BAO



Planck Clusters vs. CMB?

Planck 2013 results. XX. Cosmology from Sunyaev–Zeldovich cluster counts - arXiv:1303.5080

Assuming a bias between the X-ray determined mass and the true mass of 20%, motivated by comparison of the observed mass scaling relations to those from a set of numerical simulations, we find that ... $\sigma_8 = 0.77 \pm 0.02$ and $\Omega_m = 0.29 \pm 0.02$. The values of the cosmological parameters are degenerate with the mass bias, and it is found that the larger values of σ_8 and Ω_m preferred by the Planck's measurements of the primary CMB anisotropies can be accommodated by a mass bias of about 45%. Alternatively, consistency with the primary CMB constraints can be achieved by inclusion of processes that suppress power on small scales, such as a component of massive neutrinos.

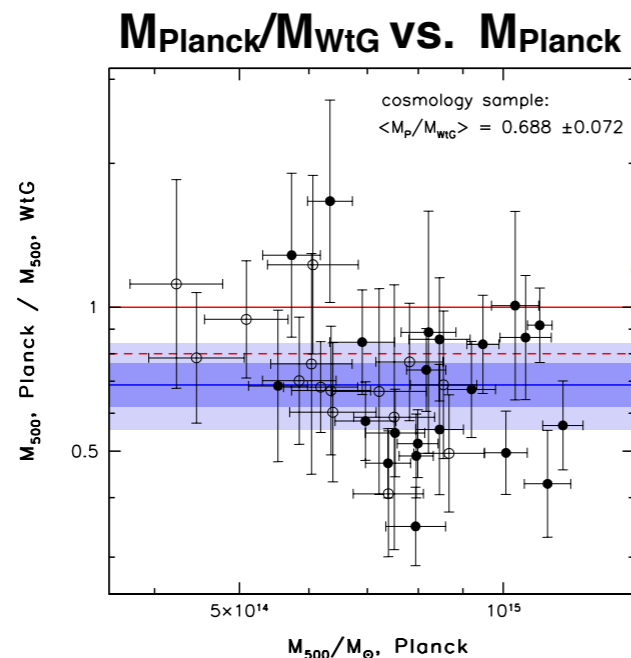
This has led to papers proposing $\Sigma m_\nu > 0.23$ eV such as Hamann & Hasenkamp JCAP 2013

Relative cluster masses can be determined accurately cluster-by-cluster using X-rays as was done by Vikhlinin+09, Mantz+10, and Planck paper XX, but the absolute masses should be calibrated using gravitational lensing, say Rozo+13,14 and van der Linden+14. The Arnaud+07,10 X-ray cluster masses used in Planck paper XX are the lowest of all. Using gravitational lensing mass calibration raises the cluster masses and thus predicts fewer expected clusters. This lessens the tension between the CMB and cluster observations.

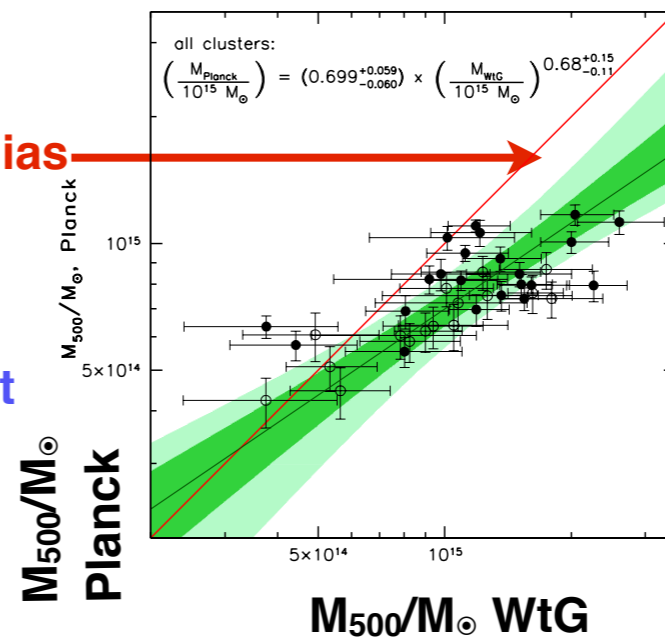
Closing the loop: self-consistent ... scaling relations for clusters of Galaxies - Rozo+14 MNRAS

Robust weak-lensing mass calibration of Planck galaxy cluster masses - von der Linden+14

The ratio of cluster masses measured by Planck and by Weighing the Giants (WtG).



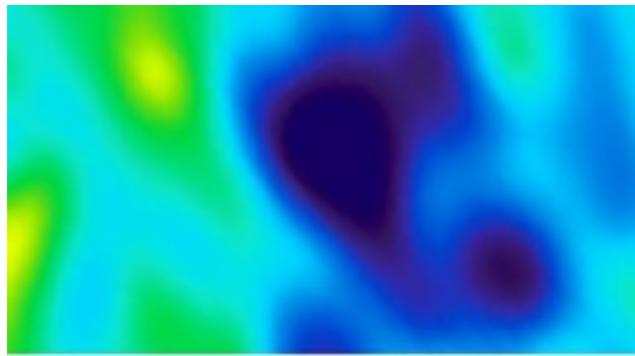
No Bias
Best Fit



M_{Planck} VS. M_{WtG}
Best Fit

This decreases the tension between clusters and CMB and the motivation for $\Sigma m_\nu > 0.23$ eV.

Late Cosmological Epochs

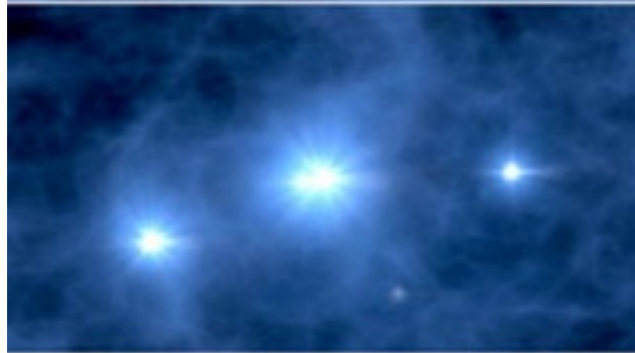


380 kyr $z \sim 1000$

recombination
last scattering



dark ages



~ 100 Myr $z \sim 30$

first stars

~ 480 Myr $z \sim 10$

"reionization"



galaxy formation

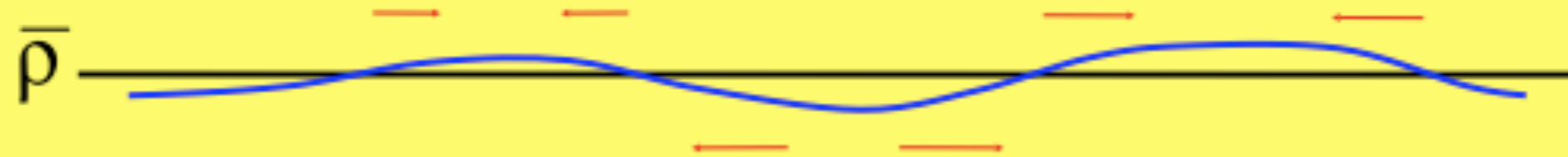


13.7 Gyr $z=0$

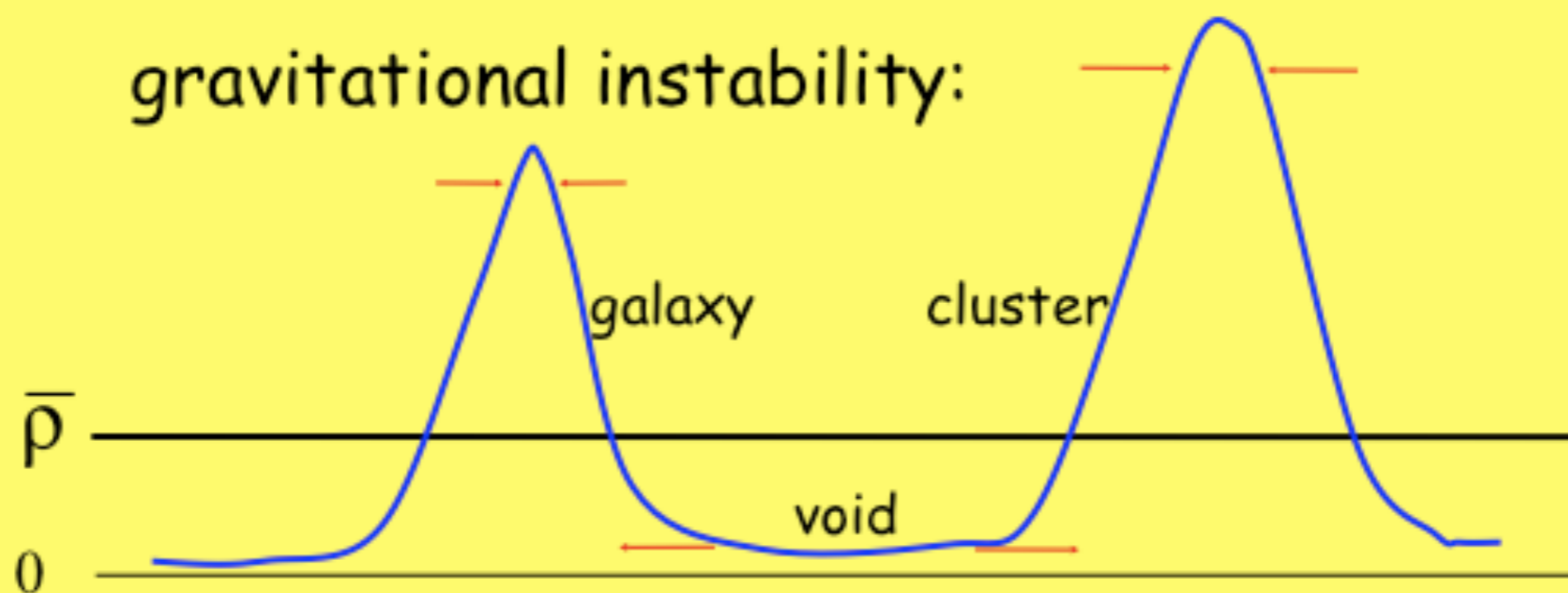
today

Gravitational instability

small-amplitude fluctuations:



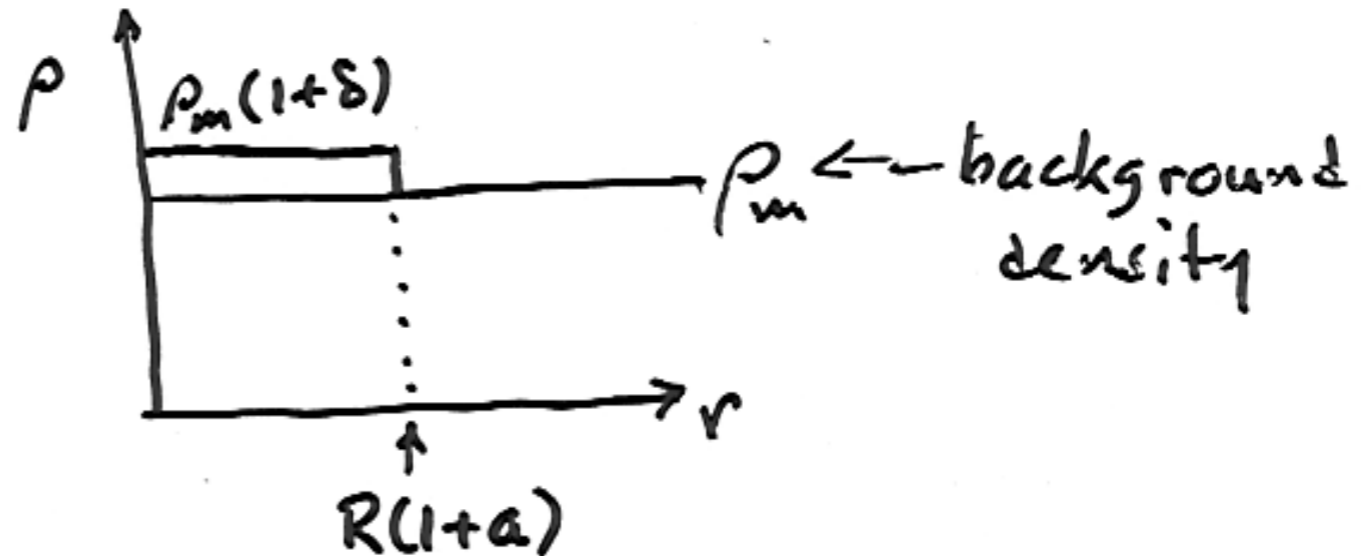
gravitational instability:



FLUCTUATIONS: LINEAR THEORY

Recall: $E(ii) - E(00) \Rightarrow \frac{2\ddot{a}}{a} = -\frac{8\pi}{3}G\rho - 8\pi Gp + \frac{2}{3}\Lambda$ (here $a = R, \Lambda=0$)

"TOP HAT MODEL"



MASS CONS. \Rightarrow

$$\rho_m(1+\delta)R^3(1+a)^3 = \text{const.} \Rightarrow$$

$$\delta = -3a$$

GRAVITY: $\ddot{R} = -\frac{4\pi G}{3}(\rho + 3p)R$

$$\ddot{\delta} + 2\frac{\dot{R}}{R}\dot{\delta} = 4\pi G\rho_m\delta$$

RAD ERA $\dot{R}/R = \frac{1}{2}t^{-1}$,
 MATTER ERA $= \frac{2}{3}t^{-1}$,

APPLIED BOTH TO FLUCT. + BCG. \Rightarrow

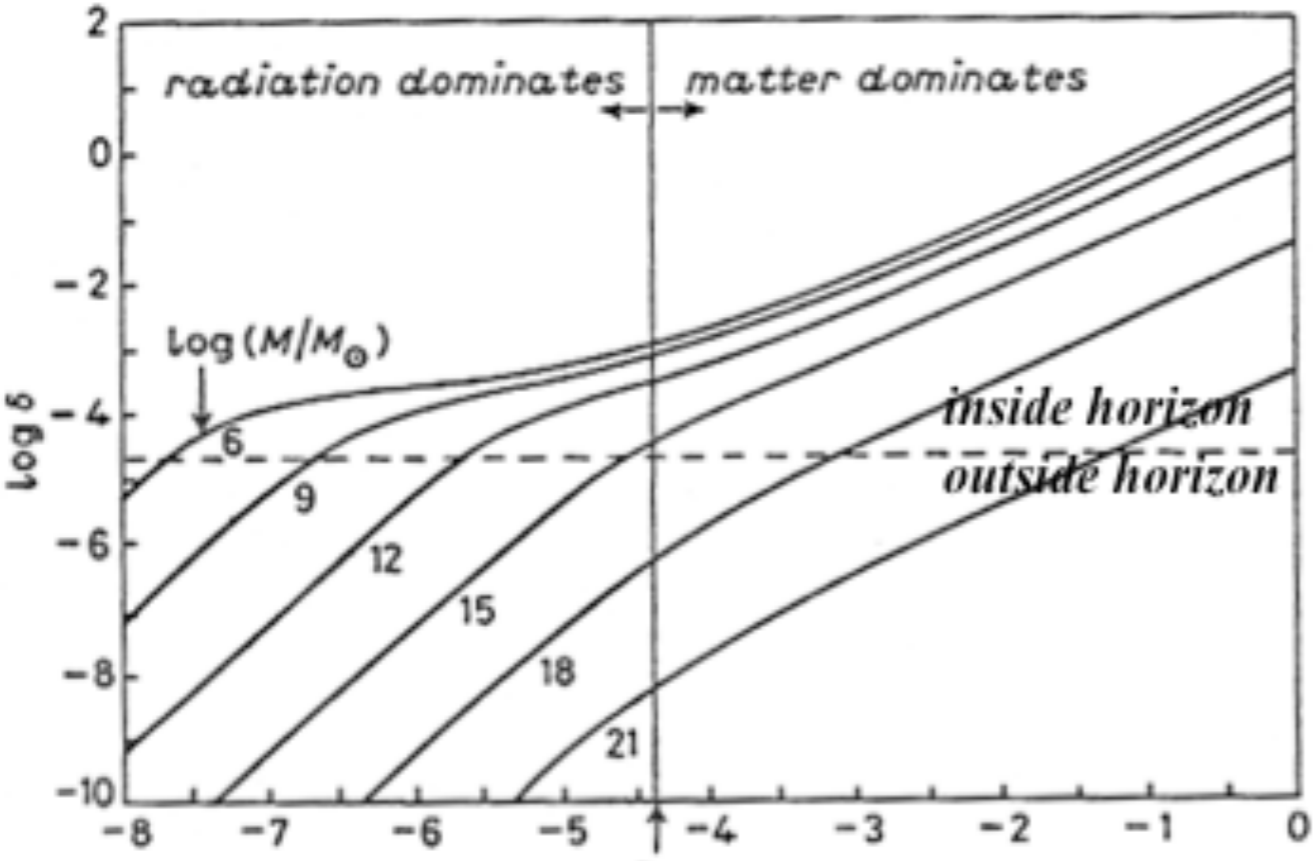
Try $\delta = t^\alpha$

$$\delta = At + Bt^{-1} = \underline{AR^2} + BR^{-2}$$

$$\delta = At^{2/3} + Bt^{-1} = \underline{AR} + BR^{-3/2}$$

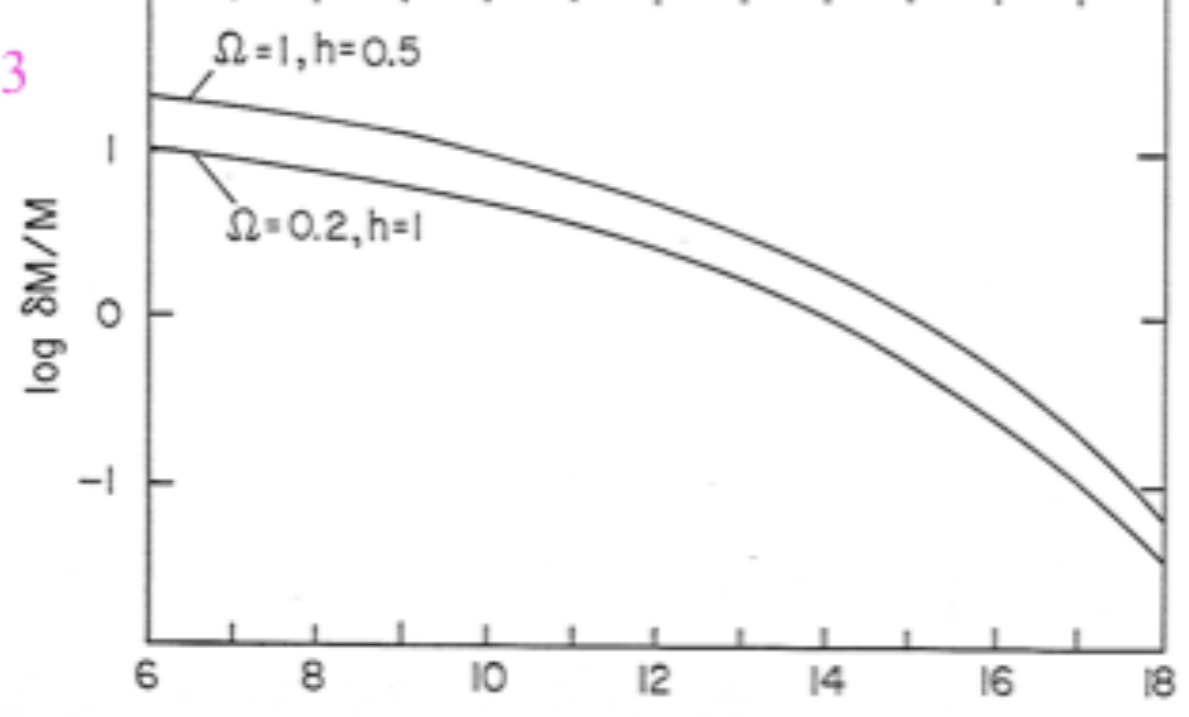
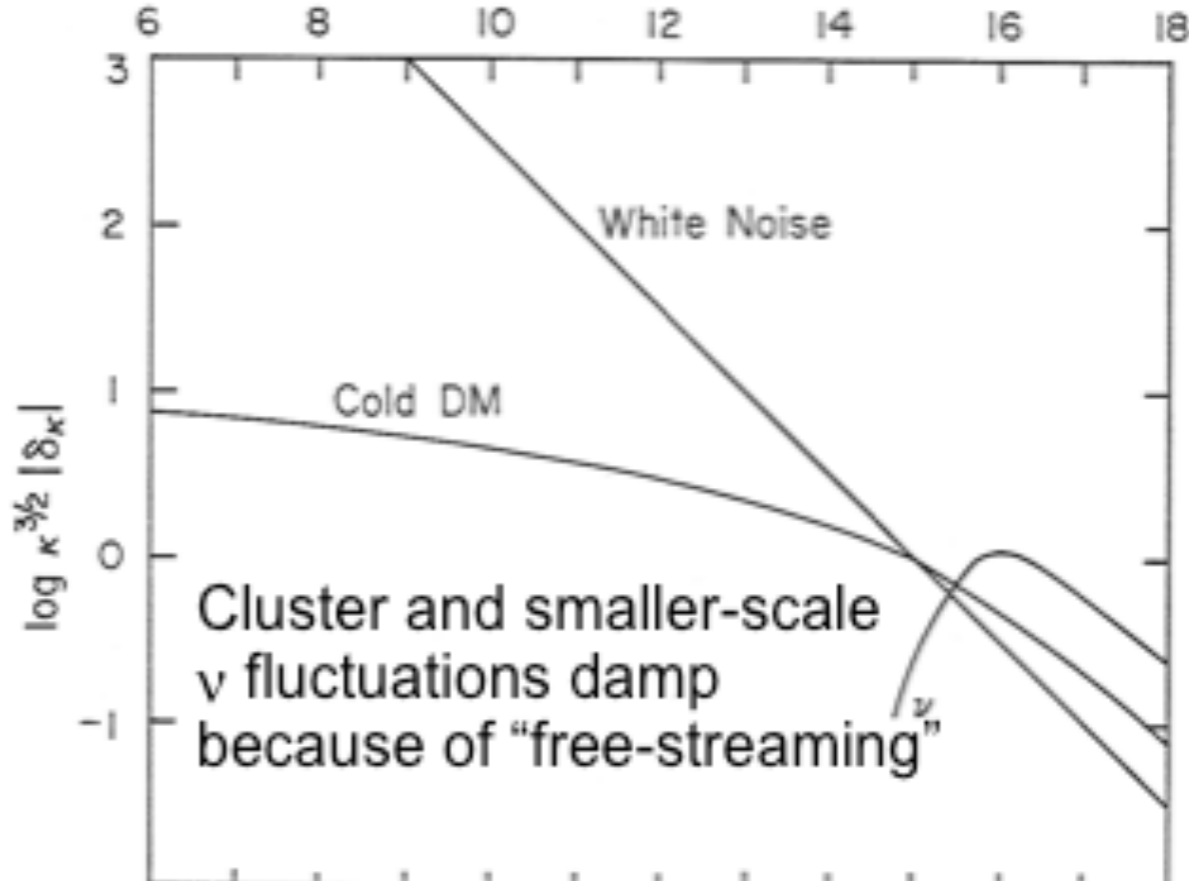
GROWING MODE

CDM Structure Formation: Linear Theory



Primack & Blumenthal 1983

Matter fluctuations that enter the horizon during the radiation dominated era, with masses less than about $10^{15} M_{\odot}$, grow only $\propto \log a$, because they are not in the gravitationally dominant component. But matter fluctuations that enter the horizon in the matter-dominated era grow $\propto a$. This explains the characteristic shape of the CDM fluctuation spectrum, with $\delta(k) \propto k^{-n/2-2} \log k$ for $k \gg k_{eq}$.



Blumenthal, Faber, Primack, & Rees 1984

The Initial Fluctuations

At Inflation: Gaussian, adiabatic

Fourier transform:

$$\delta(\vec{x}) = \sum_{\vec{k}} \delta_{\vec{k}} e^{i\vec{k}\cdot\vec{x}}$$

Power Spectrum:

$$P(k) \equiv \langle |\tilde{\delta}(\vec{k})|^2 \rangle \propto k^n$$

rms perturbation:

$$\delta_{rms} = \langle \delta^2 \rangle^{1/2} \propto \int_{k=0}^{k_{max}} P_k d^3k \propto M^{-(n+3)/6}$$

Correlation function:

$$\xi(r) \equiv \langle \delta(\vec{x})\delta(\vec{x} + \vec{r}) \rangle \propto \int |\tilde{\delta}(\vec{k})|^2 e^{-i\vec{k}\cdot\vec{r}} d^3k \propto r^{-(n+3)}$$

$$dP = [1 + \xi(r)] n dV$$

Gravitational Instability: Dark Matter

Small fluctuations: $\delta, v, \varphi(x, t)$ comoving coordinates

$$r = a(t)x \text{ etc.}$$

Continuity:

$$\dot{\delta} + \nabla \cdot v + \nabla \cdot (v\delta) = 0$$

$$H \equiv \dot{a}/a, \quad \Omega(t)$$

Euler:

$$\dot{v} + 2Hv + (v \cdot \nabla)v = -\nabla\varphi$$

matter era

Poisson:

$$\nabla^2\varphi = (3/2)H^2\Omega\delta$$

Linear approximation:

$$\ddot{\delta} + 2H\dot{\delta} = (3/2)H^2\Omega\delta$$

growing mode:

$$\delta \propto D(t) = t^{2/3} \xrightarrow{\Omega_m \rightarrow 0} t^0$$

$$\delta = -\nabla \cdot v / [Hf(\Omega)]$$

$$f(\Omega) \equiv \dot{D}/(HD) \approx \Omega^{0.6}$$

irrotational, potential flow:

$$\nabla \times v = 0 \quad v = -\nabla\varphi_v$$

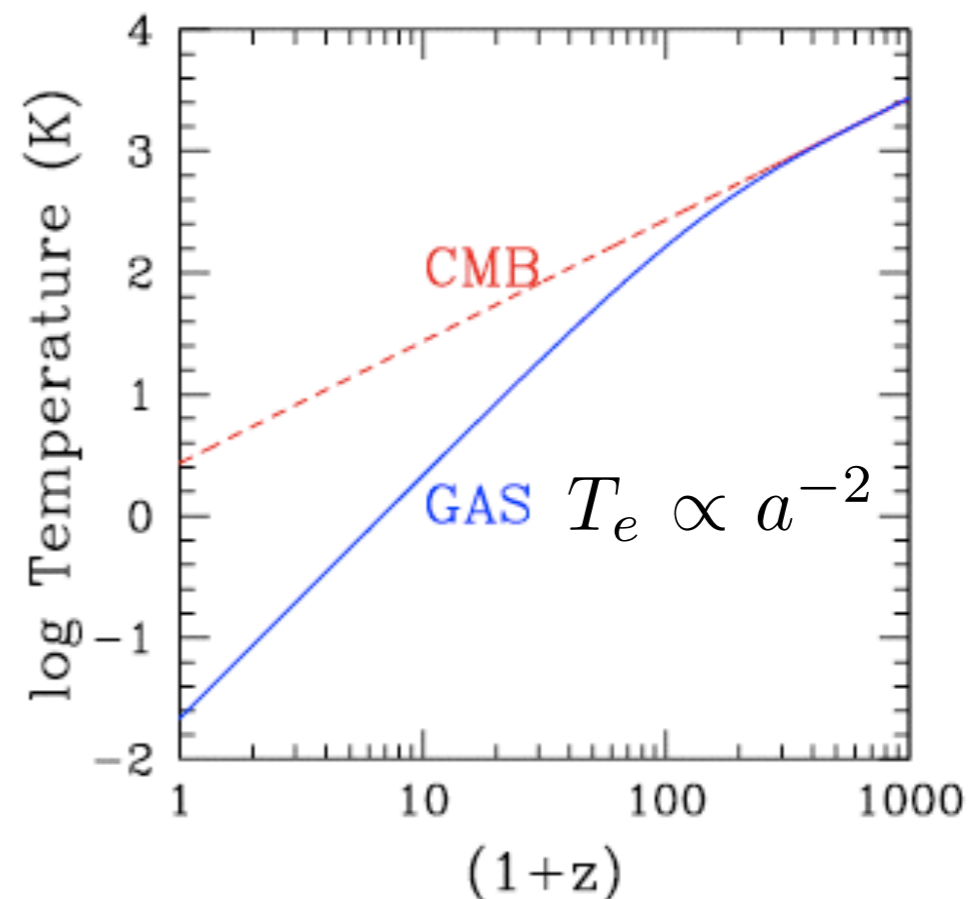
Thus far, we have considered only the evolution of fluctuations in the dark matter. But of course we have to consider also the ordinary matter, known in cosmology as “baryons” (implicitly including the electrons). See Madau’s lectures “The Astrophysics of Early Galaxy Formation” (<http://arxiv.org/abs/0706.0123v1>) for a summary. We have already seen that the baryons are primarily in the form of atoms after $z \sim 1000$, with a residual ionization fraction of a few $\times 10^{-4}$. They become fully reionized by $z \sim 6$, but they were not reionized at $z \sim 20$ since the COBE satellite found that “Compton parameter” $y \leq 1.5 \times 10^{-5}$, where

$$y = \int_0^z \frac{k_B T_e}{m_e c^2} \frac{d\tau_e}{dz} dz \quad \text{with} \quad (n_e \sigma_T c dt) = d\tau_e, \quad \sigma_T = (8\pi/3)(e^2/mc^2)^2$$

This implies that $\langle x_e T_e \rangle [(1+z)^{3/2} - 1] < 4 \times 10^7 \text{ K}$. Thus, for example, a universe that was reionized and reheated at $z = 20$ to $(x_e, T_e) = (1, > 4 \times 10^5 \text{ K})$ would violate the COBE y -limit.

The figure at right shows the evolution of the radiation (dashed line, labeled **CMB**) and matter (solid line, labeled **GAS**) temperatures after recombination, in the absence of any reheating mechanism.

(From Madau’s lectures, at physics.ucsc.edu/~joel/Phys224.)



The linear evolution of sub-horizon density perturbations in the dark matter-baryon fluid is governed in the matter-dominated era by two second-order differential equations:

$$\ddot{\delta}_{\text{dm}} + 2H\dot{\delta}_{\text{dm}} = \frac{3}{2}H^2\Omega_m^z (f_{\text{dm}}\delta_{\text{dm}} + f_b\delta_b) \quad (1)$$

for the dark matter, and

$$\ddot{\delta}_b + 2H\dot{\delta}_b = \frac{3}{2}H^2\Omega_m^z (f_{\text{dm}}\delta_{\text{dm}} + f_b\delta_b) - \frac{c_s^2}{a^2}k^2\delta_b$$

for the baryons, where $\delta_{\text{dm}}(\mathbf{k})$ and $\delta_b(\mathbf{k})$ are the Fourier components of the density fluctuations in the dark matter and baryons,† f_{dm} and f_b are the corresponding mass fractions, c_s is the gas sound speed, k is the (comoving) wavenumber, and the derivatives are taken with respect to cosmic time. Here

$$\Omega_m^z \equiv 8\pi G\rho(t)/3H^2 = \Omega_m(1+z)^3/[\Omega_m(1+z)^3 + \Omega_\Lambda] \quad (2)$$

is the time-dependent matter density parameter, and $\rho(t)$ is the total background matter density. Because there is ~ 5 times more dark matter than baryons, it is the former that defines the pattern of gravitational wells in which structure formation occurs. In the case where $f_b \approx 0$ and the universe is static ($H = 0$), equation (1) above becomes

† For each fluid component ($i = b, \text{dm}$) the real space fluctuation in the density field,

$\delta_i(\mathbf{x}) \equiv \delta\rho_i(\mathbf{x})/\rho_i$, can be written as a sum over Fourier modes,

$\delta_i(\mathbf{x}) = \int d^3\mathbf{k} (2\pi)^{-3} \delta_i(\mathbf{k}) \exp i\mathbf{k}\cdot\mathbf{x}$.

$$\ddot{\delta}_{\text{dm}} = 4\pi G\rho\delta_{\text{dm}} \equiv \frac{\delta_{\text{dm}}}{t_{\text{dyn}}^2},$$

where t_{dyn} denotes the dynamical timescale. This equation has the solution

$$\delta_{\text{dm}} = A_1 \exp(t/t_{\text{dyn}}) + A_2 \exp(-t/t_{\text{dyn}}).$$

After a few dynamical times, only the exponentially growing term is significant: gravity tends to make small density fluctuations in a static pressureless medium grow exponentially with time. Sir James Jeans (1902) was the first to discuss this.

The additional term $\propto H\dot{\delta}_{\text{dm}}$ present in an expanding universe can be thought as a “**Hubble friction**” term that acts to slow down the growth of density perturbations. Equation (1) admits the general solution for the growing mode:

$$\delta_{\text{dm}}(a) = \frac{5\Omega_m}{2} H_0^2 H \int_0^a \frac{da'}{(\dot{a}')^3}, \quad (3)$$

so that an Einstein-de Sitter universe gives the familiar scaling $\delta_{\text{dm}}(a) = a$ with coefficient unity. The right-hand side of equation (3) is called the linear growth factor $D(a) = D_+(a)$. Different values of Ω_m, Ω_Λ lead to different linear growth factors.

Growing modes actually decrease in density, but not as fast as the average universe. Note how, in contrast to the exponential growth found in the static case, the growth of perturbations even in the case of an Einstein-de Sitter ($\Omega_m = 1$) universe is just algebraic rather than exponential. This was discovered by the Russian physicist Lifshitz (1946).

Since cosmological curvature is at most marginally important at the present epoch, it was negligible during the radiation-dominated era and at least the beginning of the matter-dominated era. But for $k = -1$, i.e. $\Omega < 1$, the growth of δ slows for $(R/R_o) \gtrsim \Omega_o$, as gravity becomes less important and the universe begins to expand freely. To discuss this case, it is convenient to introduce the variable

$$x \equiv \Omega^{-1}(t) - 1 = (\Omega_o^{-1} - 1)R(t)/R_o. \quad (2.55)$$

(Note that $\Omega(t) \rightarrow 1$ at early times.) The general solution in the matter-dominated era is then (Peebles, 1980, §11)

$$\delta = \tilde{A}D_1(t) + \tilde{B}D_2(t), \quad (2.56)$$

where the growing solution is

$$D_1 = 1 + \frac{3}{x} + \frac{3(1+x)^{1/2}}{x^{3/2}} \ln \left[(1+x)^{1/2} - x^{1/2} \right] \quad (2.57)$$

and the decaying solution is

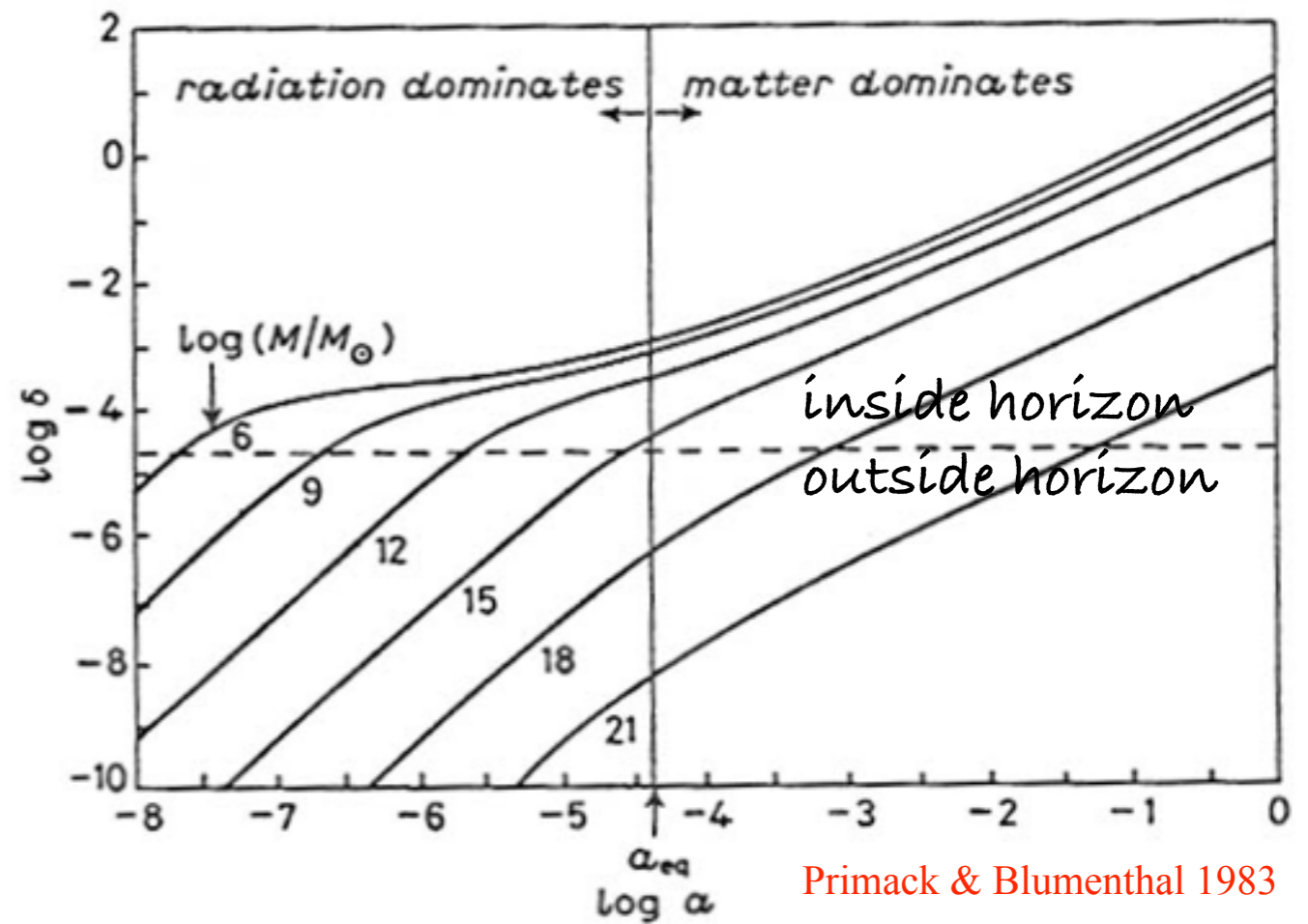
$$D_2 = (1+x)^{1/2}/x^{3/2}. \quad (2.58)$$

These agree with the Einstein-de Sitter results (2.53) at early times ($t \ll t_o, x \ll 1$). For late times ($t \gg t_o, x \gg 1$) the solutions approach

$$D_1 = 1, D_2 = x^{-1}; \quad (2.59)$$

in this limit the universe is expanding freely and the amplitude of fluctuations stops growing.

The consequence is that dark matter fluctuations grow proportionally to the scale factor $a(t)$ when matter is the dominant component of the universe, but only logarithmically when radiation is dominant. Thus there is not much difference in the amplitudes of fluctuations of mass $M < 10^{15} M_{\text{sun}}$, which enter the horizon before $z_{\text{mr}} \sim 4 \times 10^3$, while there is a stronger dependence on M for fluctuations with $M > 10^{15} M_{\text{sun}}$.



There is a similar suppression of the growth of matter fluctuations once the gravitationally dominant component of the universe is the dark energy, for example a cosmological constant. Lahav, Lilje, Primack, & Rees (1991) showed that the growth factor in this case is well approximated by

$$\delta_{\text{dm}}(a) = D(a) \simeq \frac{5\Omega_m^z}{2(1+z)} \left[(\Omega_m^z)^{4/7} - \frac{(\Omega_m^z)^2}{140} + \frac{209}{140}\Omega_m^z + \frac{1}{70} \right]^{-1}.$$

Here Ω_m^z is again given by $\Omega_m^z \equiv 8\pi G\rho(t)/3H^2 = \Omega_m(1+z)^3/[\Omega_m(1+z)^3 + \Omega_\Lambda]$

The Linear Transfer Function $T(k)$

The observed uniformity of the CMB guarantees that density fluctuations must have been quite small at decoupling, implying that the evolution of the density contrast can be studied at $z \lesssim z_{\text{dec}}$ using linear theory, and each mode $\delta(k)$ evolves independently. The inflationary model predicts a scale-invariant primordial power spectrum of density fluctuations $P(k) \equiv \langle |\delta(k)|^2 \rangle \propto k^n$, with $n = 1$ (the so-called Harrison-Zel'dovich spectrum). It is the index n that governs the balance between large and small-scale power. In the case of a Gaussian random field with zero mean, the power spectrum contains the complete statistical information about the density inhomogeneity. It is often more convenient to use the dimensionless quantity $\Delta_k^2 \equiv [k^3 P(k)/2\pi^2]$, which is the power per logarithmic interval in wavenumber k . In the matter-dominated epoch, this quantity retains its initial primordial shape ($\Delta_k^2 \propto k^{n+3}$) only on very large scales. Small wavelength modes enter the horizon earlier on and their growth is suppressed more severely during the radiation-dominated epoch: on small scales the amplitude of Δ_k^2 is essentially suppressed by four powers of k (from k^{n+3} to k^{n-1}). If $n = 1$, then small scales will have nearly the same power except for a weak, logarithmic dependence. Departures from the initially scale-free form are described by the transfer function $T(k)$, defined such that $T(0) = 1$:

$$P(k, z) = Ak^n \left[\frac{D(z)}{D(0)} \right]^2 T^2(k),$$

where A is the normalization.

An approximate fitting function for $T(k)$ in a Λ CDM universe is (Bardeen et al. 1986)

$$T_k = \frac{\ln(1 + 2.34q)}{2.34q} [1 + 3.89q + (16.1q)^2 + (5.46q)^3 + (6.71q)^4]^{-1/4},$$

where (Sugayama 1995)

$$q \equiv \frac{k/\text{Mpc}^{-1}}{\Omega_m h^2 \exp(-\Omega_b - \Omega_b/\Omega_m)}.$$

For accurate work, for example for starting high-resolution N-body simulations, it is best to use instead of fitting functions the numerical output of highly accurate integration of the Boltzmann equations, for example from CMBFast, which is available at <http://lambda.gsfc.nasa.gov/toolbox/> which points to http://lambda.gsfc.nasa.gov/toolbox/tb_cmbfast_ov.cfm

W e l c o m e to the CMBFAST Website!

This is the most extensively used code for computing cosmic microwave background anisotropy, polarization and matter power spectra. The code has been tested over a wide range of cosmological parameters. We are continuously testing and updating the code based on suggestions from the cosmological community. Do not hesitate to contact us if you have any questions or suggestions.

U. Seljak & M. Zaldarriaga

CMB Toolbox Overview

We provide links to a number of useful tools for CMB and Astronomy in general.

CMB Tools

- [CMB Simulations](#) - High-resolution, full-sky microwave temperature simulations including secondary anisotropies.
- [Contributed Software](#) is an archive at a LAMBDA partner site for tools built by members of the community.
- [CMBFast](#) - A tool that computes spectra for the cosmic background for a given set of CMB parameters. LAMBDA provides a [web-based interface](#) for this tool. Seljak and Zaldarriaga
- [CAMB](#) - Code for Anisotropies in the Microwave Background that computes spectra for a set of CMB parameters. LAMBDA provides a [web-based interface](#) for this tool. Lewis and Challinor
- [CMBEASY](#) - A C++ package, initially based on CMBFAST, now featuring a parameter likelihood package as well. Doran
- [CMBview](#) - A Mac OS X program for viewing HEALPix-format CMB data on an OpenGL-rendered sphere. Portsmouth
- [COMBAT](#) - A set of computational tools for CMB analysis. Borrill et al.
- [CosmoMC](#) - A Markov-Chain Monte-Carlo engine for exploring cosmological parameter space. Lewis and Bridle
- [CosmoNet](#) - Accelerated cosmological parameter estimation using Neural Networks.
- [GLESP](#) - Gauss-Legendre sky pixelization package. Doroshkevich, et al.
- [GSM](#) - Predicted all-sky maps at any frequency from 10 MHz to 100 GHz. de Oliveira-Costa.
- [HEALPix](#) - A spherical sky pixelization scheme. The Wilkinson Microwave Anisotropy Probe (WMAP) data skymap products are supplied in this form. Górski et al.
- [IGLOO](#) - A sky pixelization package. Crittenden and Turok
- [MADCAP](#) - Microwave Anisotropy Data Computational Analysis Package. Borrill et al.
- [PICO](#) - Integrates with CAMB and/or CosmoMC for cosmological parameter estimation using machine learning. Wandelt and Fendt
- [RADPACK](#) - Radical Compression Analysis Package. Knox
- [RECFAST](#) - Software to calculate the recombination history of the Universe. Seager, Sasselov, and Scott
- [SkyViewer](#) - A LAMBDA-developed OpenGL-based program to display HEALPix-based skymaps stored in FITS format files. Phillips
- [SpiCE](#) - Spatially Inhomogenous Correlation Estimator. Szapudi et al.
- [WMAPViewer](#) - A LAMBDA-developed web-based CMB map viewing tool using a technology similar to that found on maps.google.com. Phillips
- [WOMBAT](#) - Microwave foreground emission tools. Gawiser, Finkbeiner, Jaff et al.

Likelihood Software

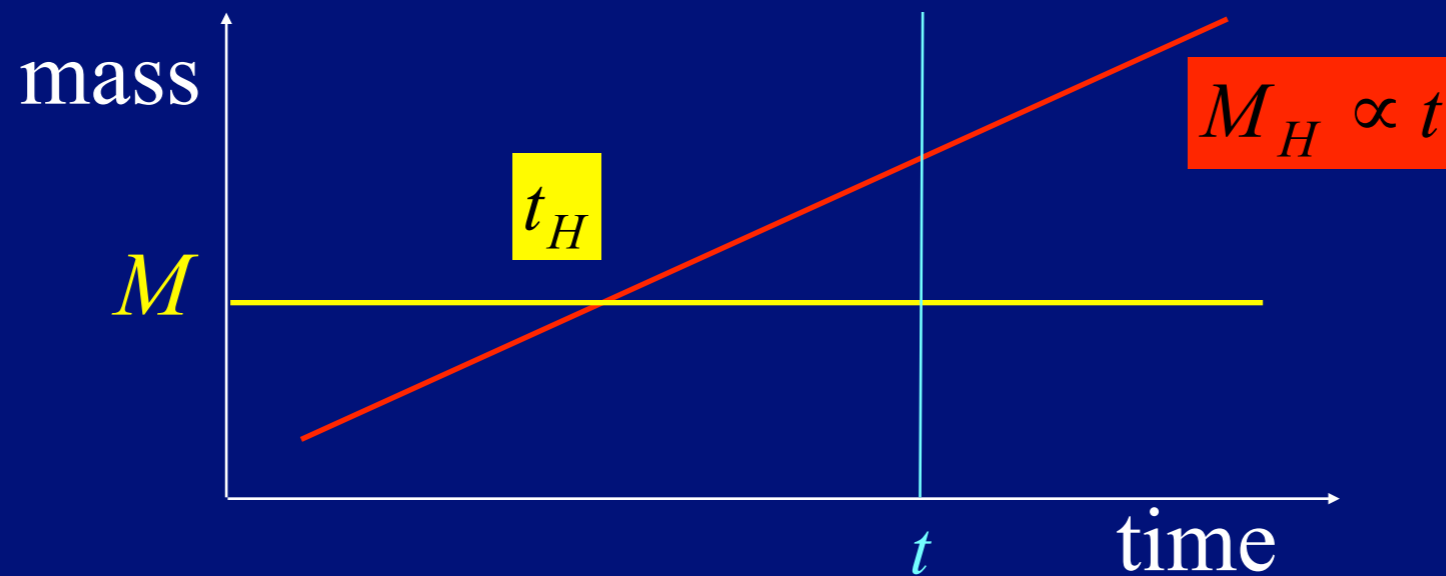
- [SDSS LRG DR7 Likelihood Software](#) - A software package that computes likelihoods for Luminous Red Galaxies (LRG) data from the seventh release of the Sloan Digital Sky Survey (SDSS).
- [WMAP Likelihood Software](#) - A software library used by the WMAP team to compute Fisher and Master matrices and to compute the likelihoods of various models. This is the same software found on the [WMAP products list](#); more information may be found [here](#).

Other Tools

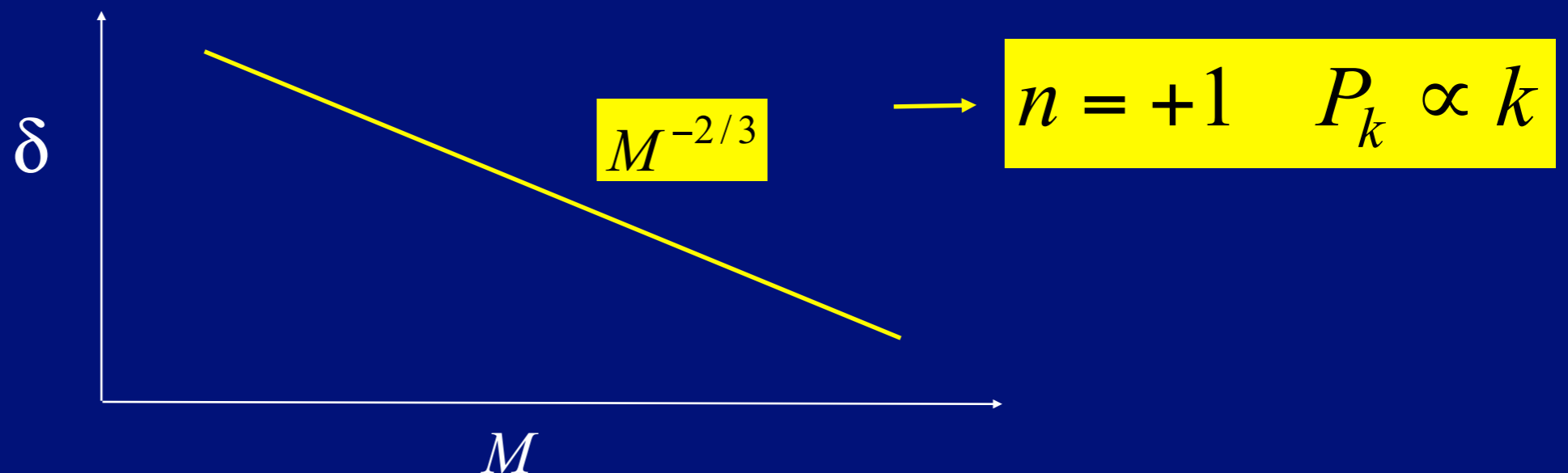
- [WMAP Effective Frequency Calculator](#) - A tool that calculates the effective frequencies of the five WMAP frequency bands.
- [CFITSIO](#) - A library of C and Fortran routines for reading and writing data in the FITS format.
- [IDL Astro](#) - The IDL Astronomy Users Library.
- [Conversion Utilities](#) - A small collection of astronomical conversion utilities.
- [Calculators](#) - A list of links to calculators.

This collection of tools can only be extended and improved with your input! Please feel free to send us [suggestions and comments](#).

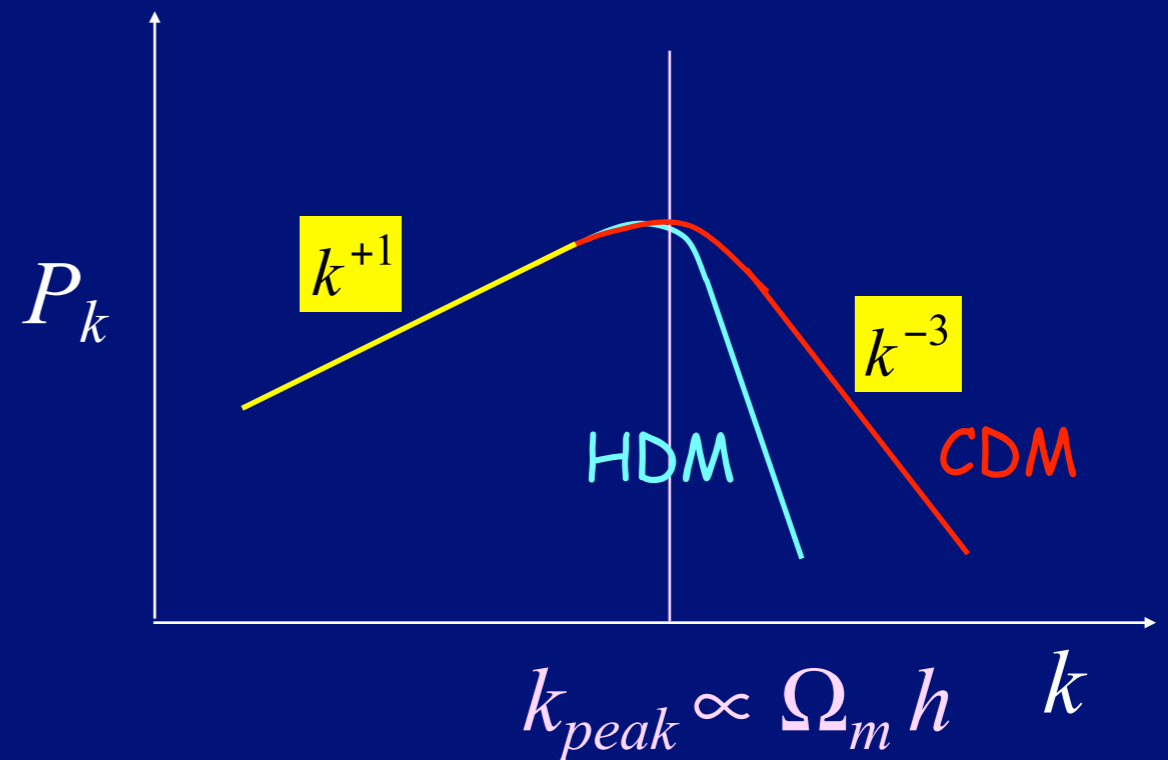
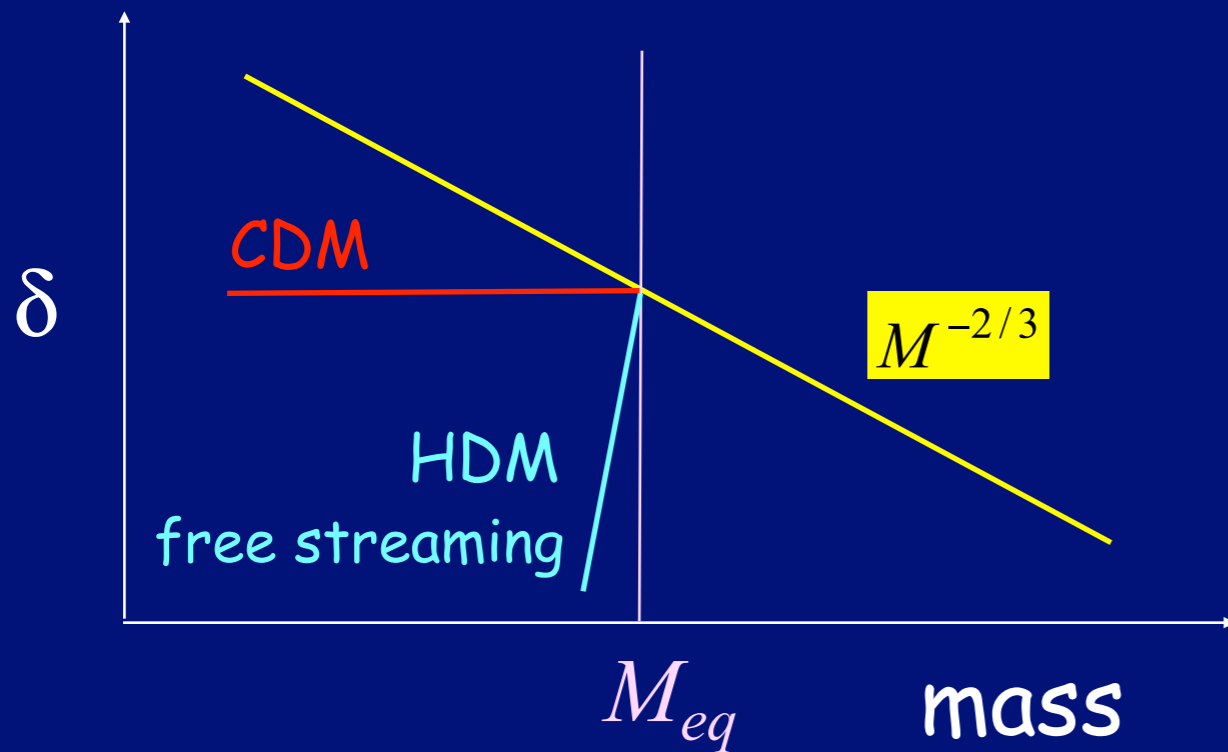
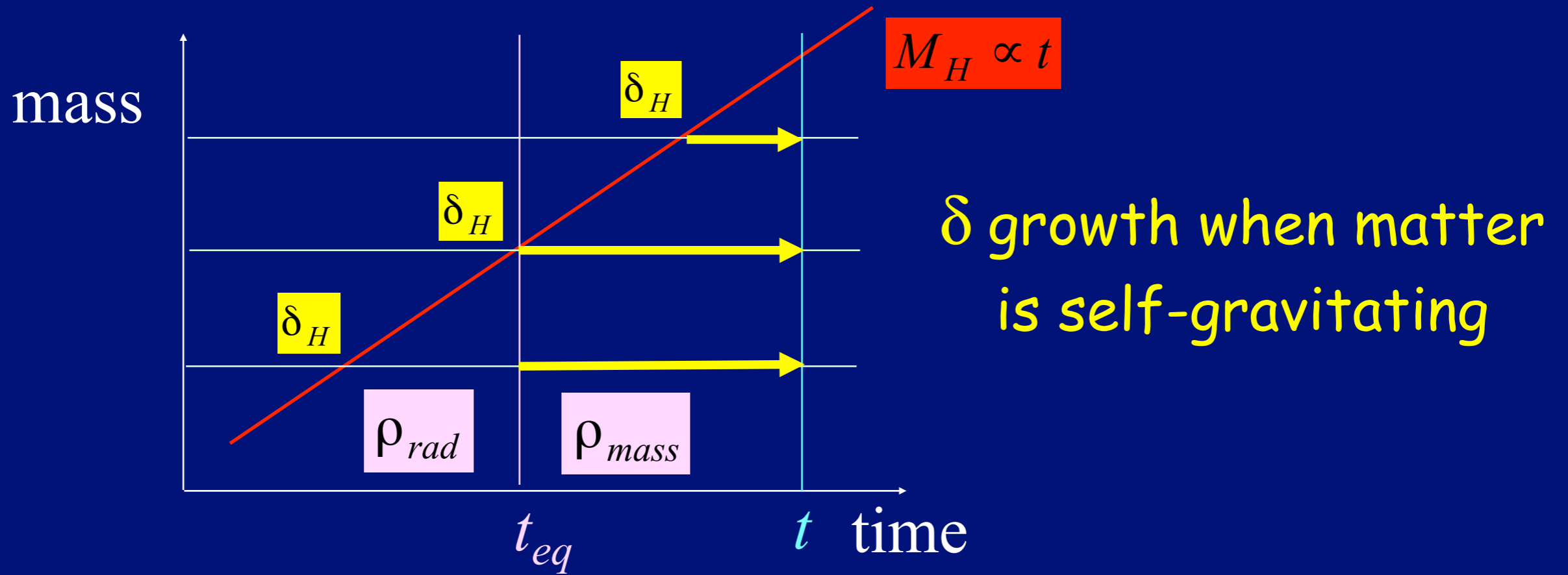
Scale-Invariant Spectrum (Harrison-Zel'dovich)



$$\delta(M, t) = \delta_H \left(\frac{t}{t_H(M)} \right)^{2/3} \propto M^{-2/3} t^{2/3}$$



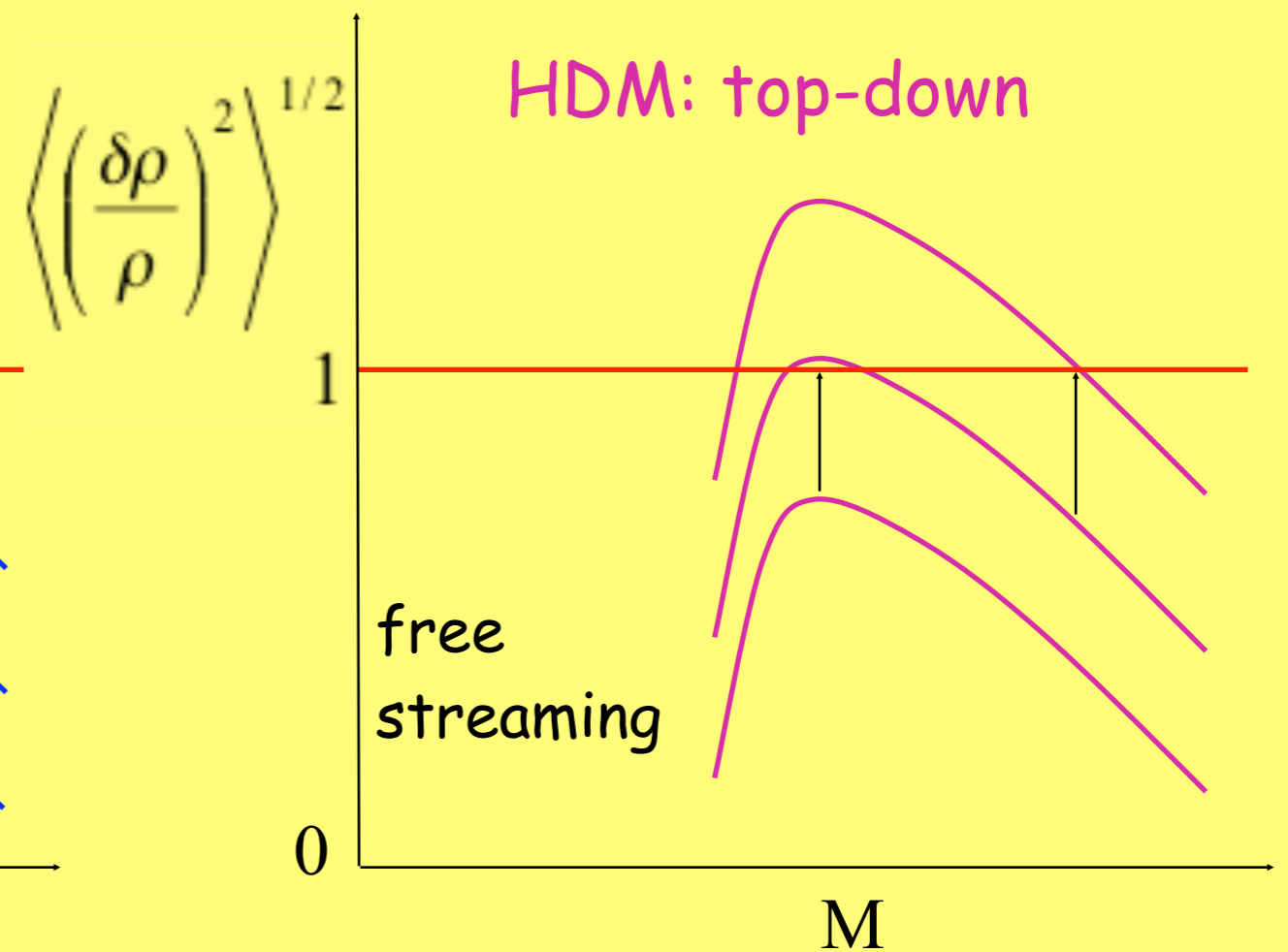
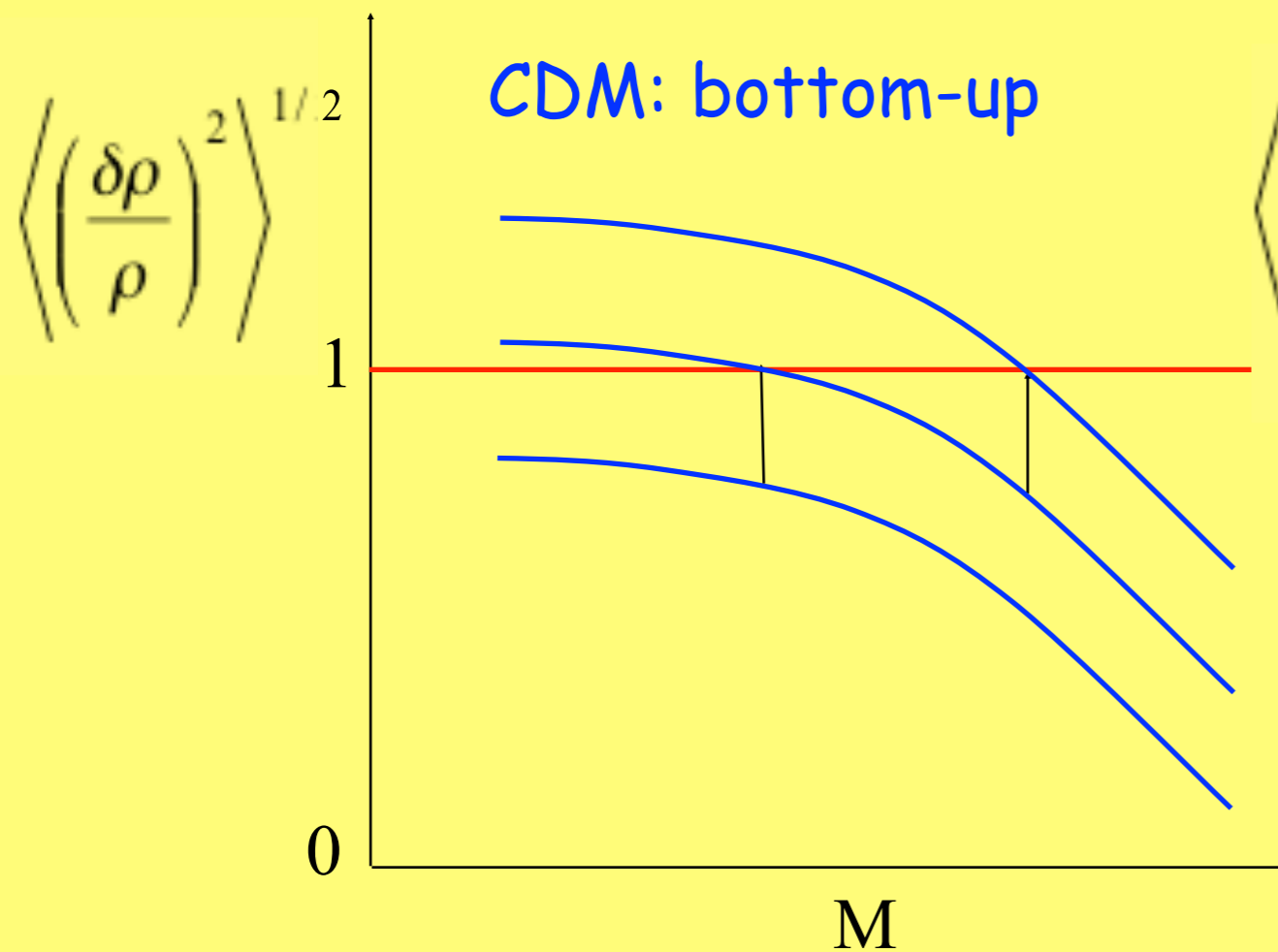
CDM Power Spectrum



Formation of Large-Scale Structure

Fluctuation growth in the linear regime: $\delta \ll 1 \longrightarrow \delta \propto t^{2/3}$

rms fluctuation at mass scale M : $\delta \propto M^{-\alpha} \quad 0 < \alpha \leq 2/3$



Galaxies Clusters Superclusters

Galaxies Clusters Superclusters

Structure forms earliest in Open, next in Benchmark, latest in EdS model.

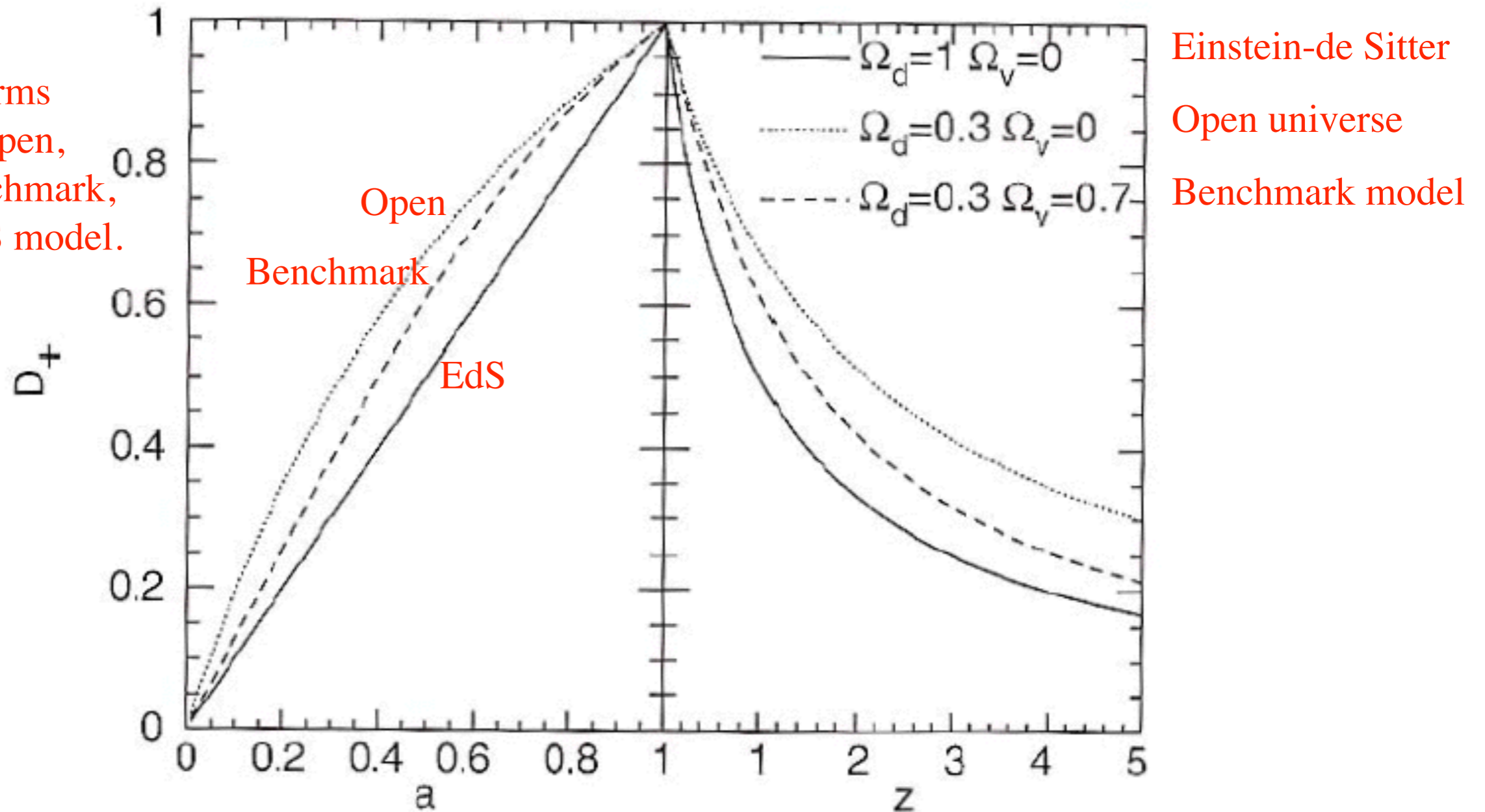


Fig. 7.3. Growth factor D_+ for three different cosmological models, as a function of the scale factor a (left panel) and of redshift (right panel). It is clearly visible how quickly D_+ decreases with increasing redshift in the EdS model, in comparison to the models of lower density

From Peter Schneider, *Extragalactic Astronomy and Cosmology* (Springer, 2006)

Linear Growth Rate Function $D(a)$

For completeness, here we present some approximations used in the text. For the family of flat cosmologies ($\Omega_m + \Omega_\Lambda = 1$) an accurate approximation for the value of the virial overdensity Δ_{vir} is given by the analytic formula (Bryan & Norman 1998):

$$\Delta_{\text{vir}} = (18\pi^2 + 82x - 39x^2)/\Omega(z), \quad (\text{A1})$$

where $\Omega(z) \equiv \rho_m(z)/\rho_{\text{crit}}$ and $x \equiv \Omega(z) - 1$.

The linear growth-rate function $\delta(a)$, used in eqs. (14-15) and also in $\sigma_8(a)$ is defined as

$$\delta(a) = D(a)/D(1), \quad (\text{A2})$$

where $a = 1/(1+z)$ is the expansion parameter and $D(a)$ is:

$$D(a) = \frac{5}{2} \left(\frac{\Omega_{m,0}}{\Omega_{\Lambda,0}} \right)^{1/3} \frac{\sqrt{1+x^3}}{x^{3/2}} \int_0^x \frac{x^{3/2} dx}{[1+x^3]^{3/2}}, \quad (\text{A3})$$

$$x \equiv \left(\frac{\Omega_{\Lambda,0}}{\Omega_{m,0}} \right)^{1/3} a, \quad (\text{A4})$$

where $\Omega_{m,0}$ and $\Omega_{\Lambda,0}$ are density contributions of matter and cosmological constant at $z = 0$. For $\Omega_m > 0.1$ the growth rate factor $D(a)$ can be accurately approximated by the following expressions (Lahav et al. 1991; Carroll et al. 1992):

$$D(a) = \frac{(5/2)a\Omega_m}{\Omega_m^{4/7} - \Omega_\Lambda + (1 + \Omega_m/2)(1 + \Omega_\Lambda/70)}, \quad (\text{A5})$$

$$\Omega_m(a) = \Omega_{m,0}/(1+x^3), \quad (\text{A6})$$

$$\Omega_\Lambda(a) = 1 - \Omega_m(a) \quad (\text{A7})$$

For $\Omega_{m,0} = 0.27$ the error of these approximation is less than 7×10^{-4} .

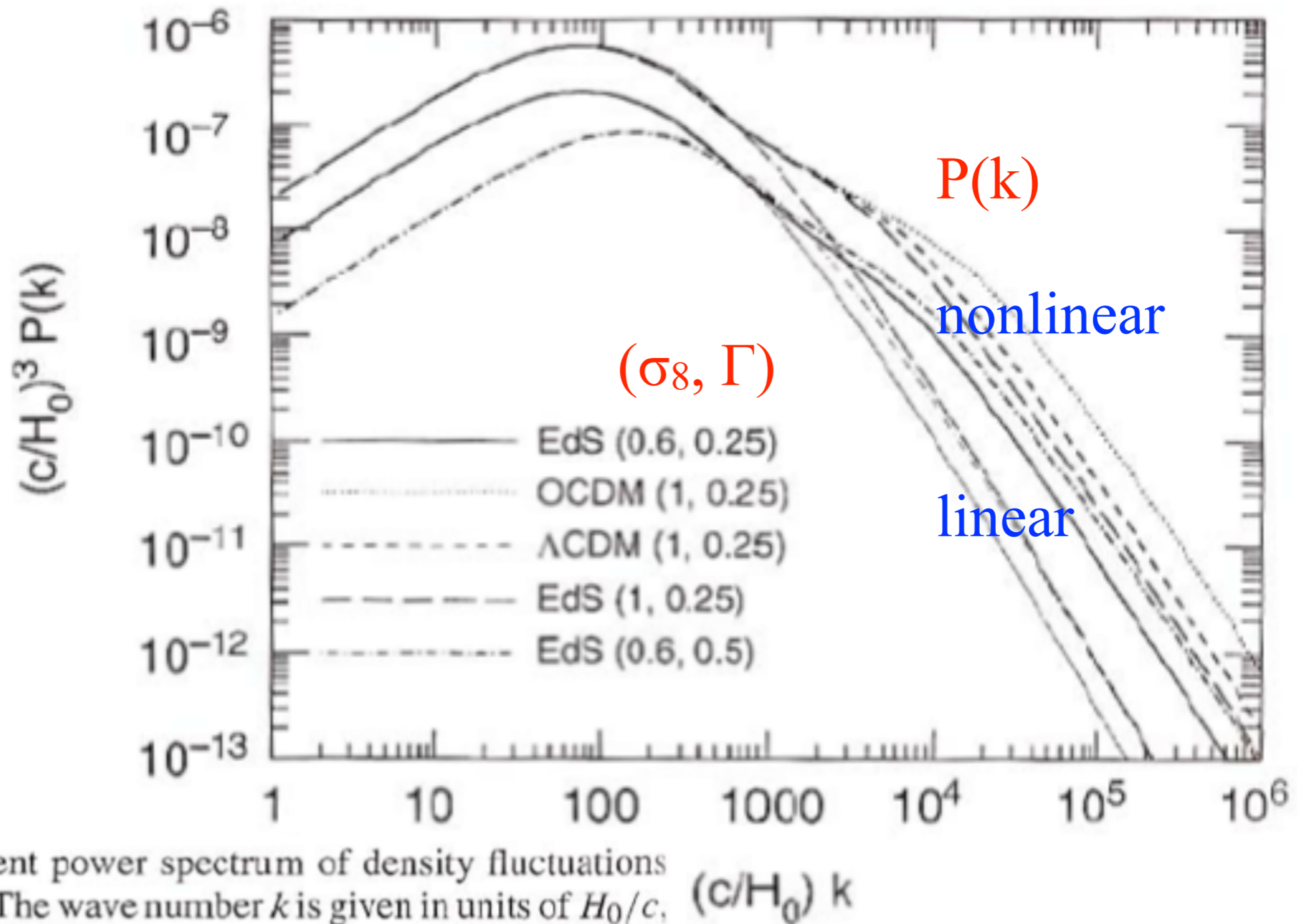


Fig. 7.6. The current power spectrum of density fluctuations for CDM models. The wave number k is given in units of H_0/c , and $(H_0/c)^3 P(k)$ is dimensionless. The various curves have different cosmological parameters: EdS: $\Omega_m = 1$, $\Omega_\Lambda = 0$; OCDM: $\Omega_m = 0.3$, $\Omega_\Lambda = 0$; Λ CDM: $\Omega_m = 0.3$, $\Omega_\Lambda = 0.7$. The values in parentheses specify (σ_8, Γ) , where σ_8 is the normalization of the power spectrum (which will be discussed below), and where Γ is the shape parameter. The thin curves correspond to the power spectrum $P_0(k)$ linearly extrapolated to the present day, and the bold curves take the non-linear evolution into account. The shape parameter $\Gamma = \Omega_m h$.

From Peter Schneider,
*Extragalactic Astronomy and
 Cosmology* (Springer, 2006)

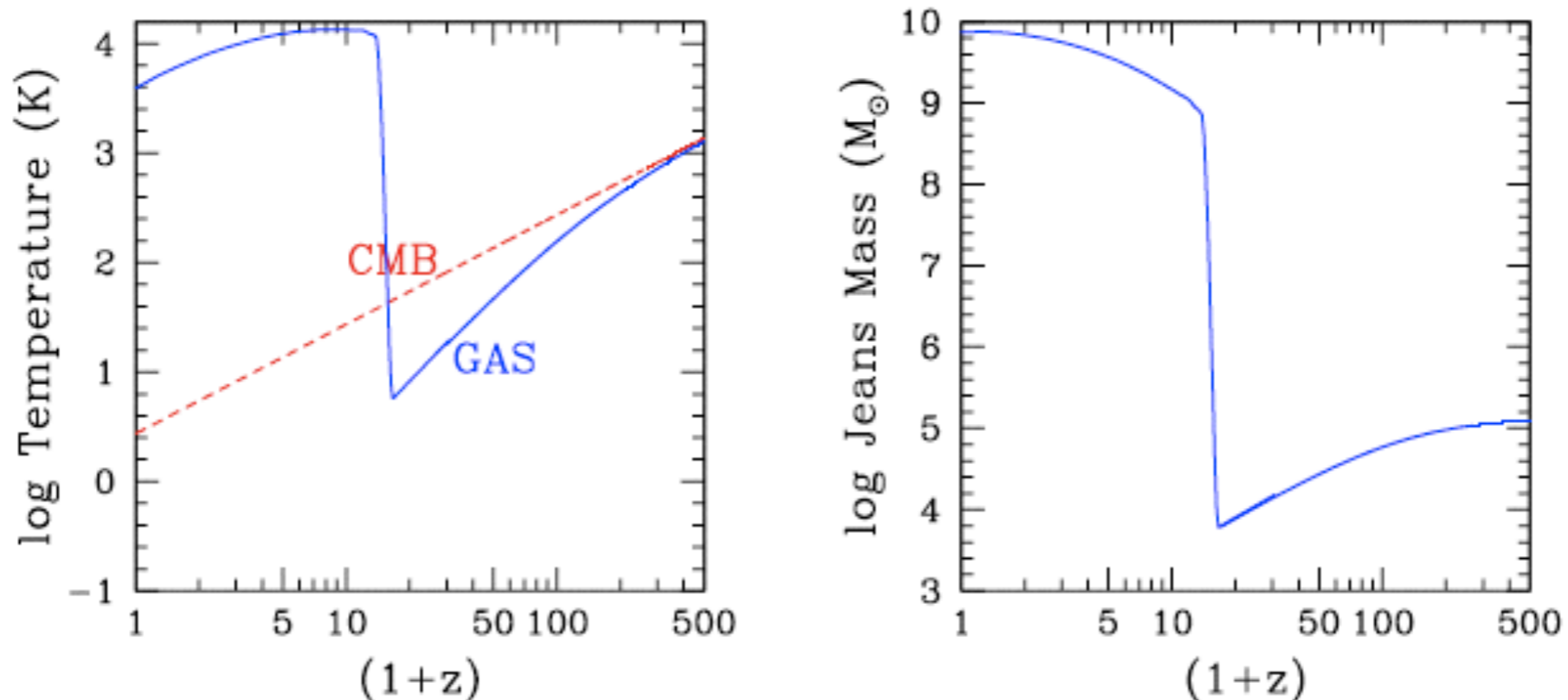
On large scales (k small), the gravity of the dark matter dominates. But on small scales, pressure dominates and growth of baryonic fluctuations is prevented. Gravity and pressure are equal at the Jeans scale

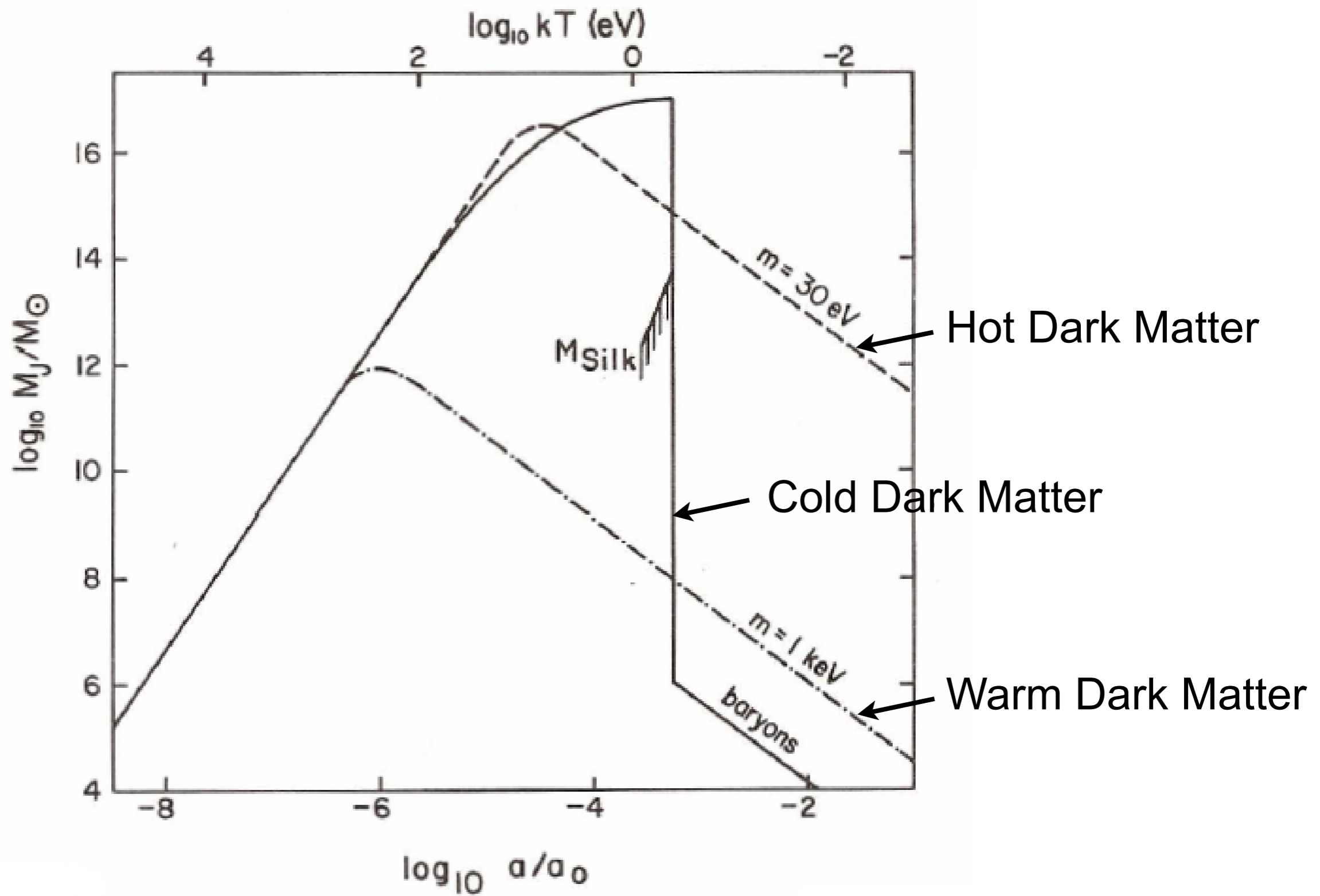
$$k_J = \frac{a}{c_s} \sqrt{4\pi G \rho}.$$

The Jeans mass is the dark matter + baryon mass enclosed within a sphere of radius $\pi a/k_J$,

$$M_J = \frac{4\pi}{3} \rho \left(\frac{\pi a}{k_J} \right)^3 = \frac{4\pi}{3} \rho \left(\frac{5\pi k_B T_e}{12G\rho m_p \mu} \right)^{3/2} \approx 8.8 \times 10^4 M_\odot \left(\frac{a T_e}{\mu} \right)^{3/2},$$

where μ is the mean molecular weight. The evolution of M_J is shown below, assuming that reionization occurs at $z=15$:

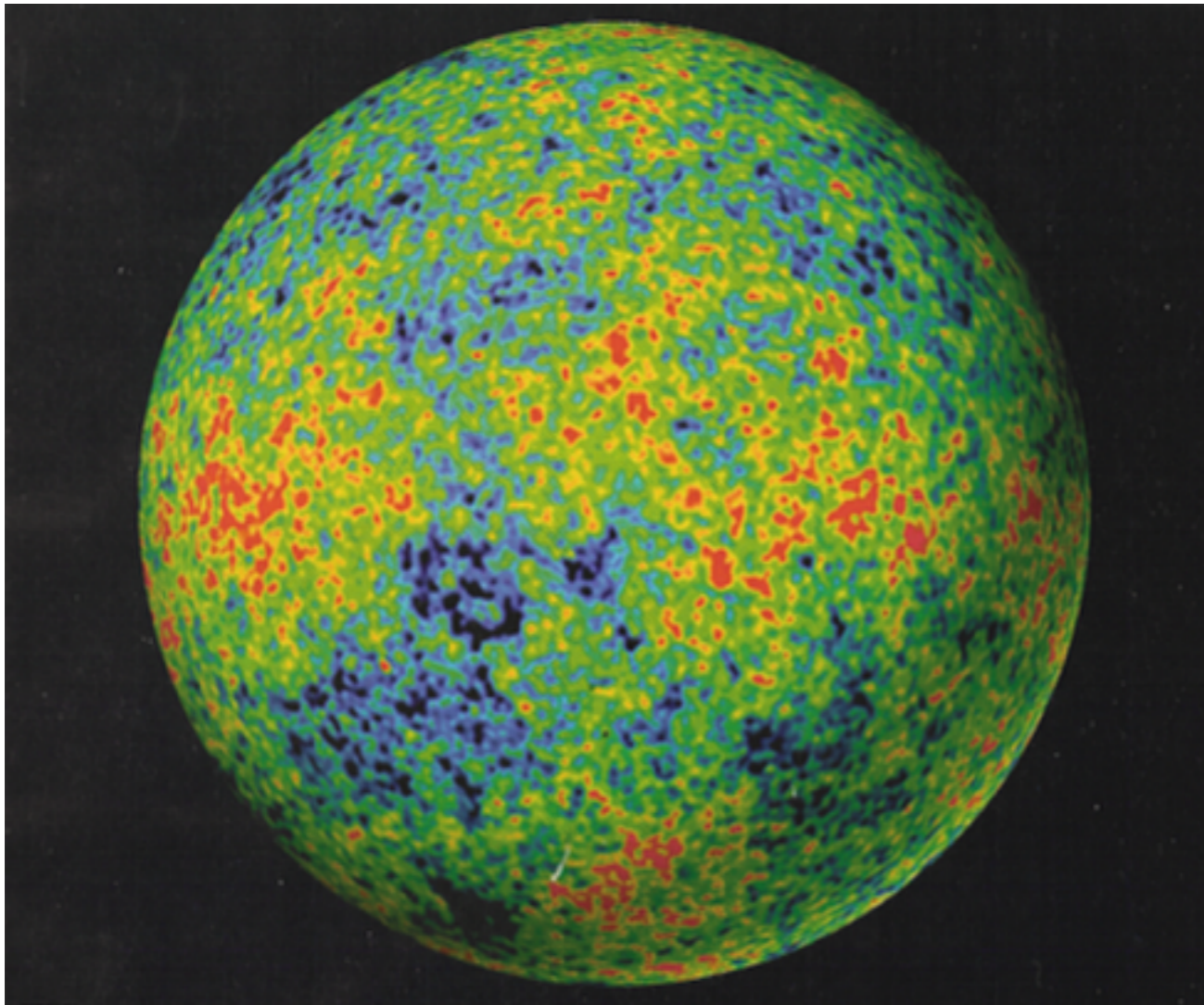




Jeans-type analysis for HDM, WDM, and CDM

GRAVITY – The Ultimate Capitalist Principle

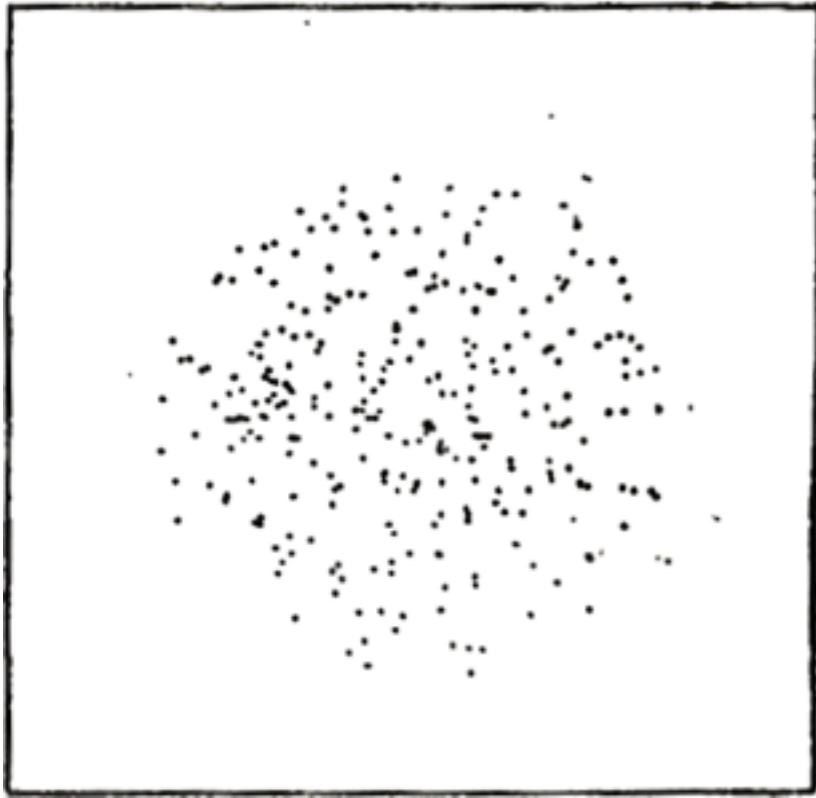
Astronomers say that a region of the universe with more matter is “richer.” Gravity magnifies differences—if one region is slightly denser than average, it will expand slightly more slowly and grow relatively denser than its surroundings, while regions with less than average density will become increasingly less dense. The rich always get richer, and the poor poorer.



The early universe expands *almost* perfectly uniformly. But there are small differences in density from place to place (about 30 parts per million). Because of gravity, denser regions expand more slowly, less dense regions more rapidly. Thus gravity amplifies the contrast between them, until...

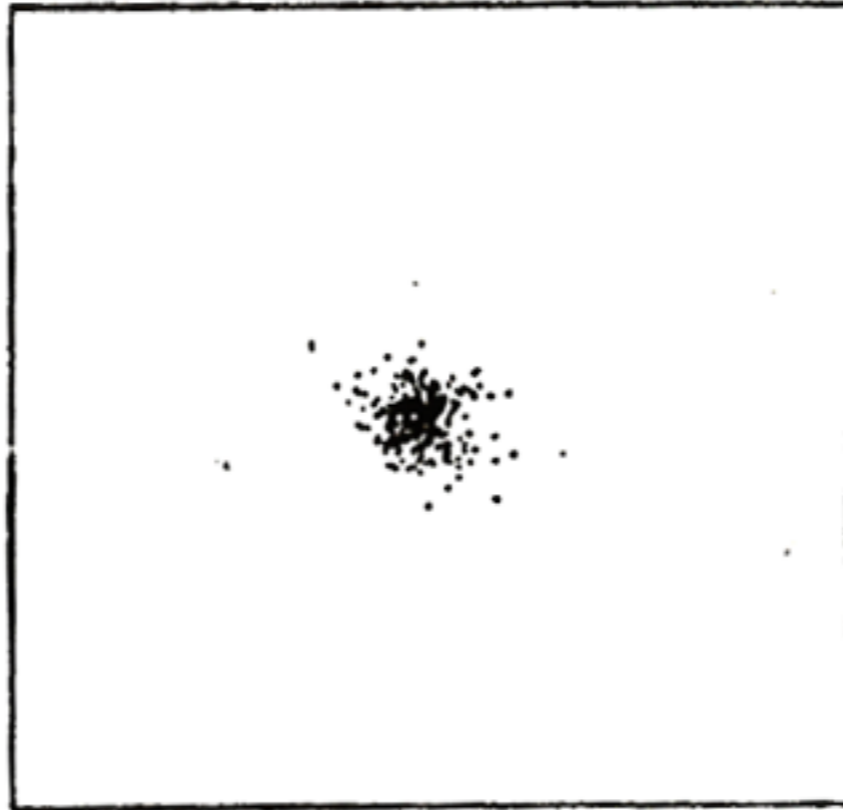
Temperature map at 380,000 years after the Big Bang. **Blue** (cooler) regions are slightly denser. From NASA's **WMAP** satellite, 2003.

Structure Formation by Gravitational Collapse



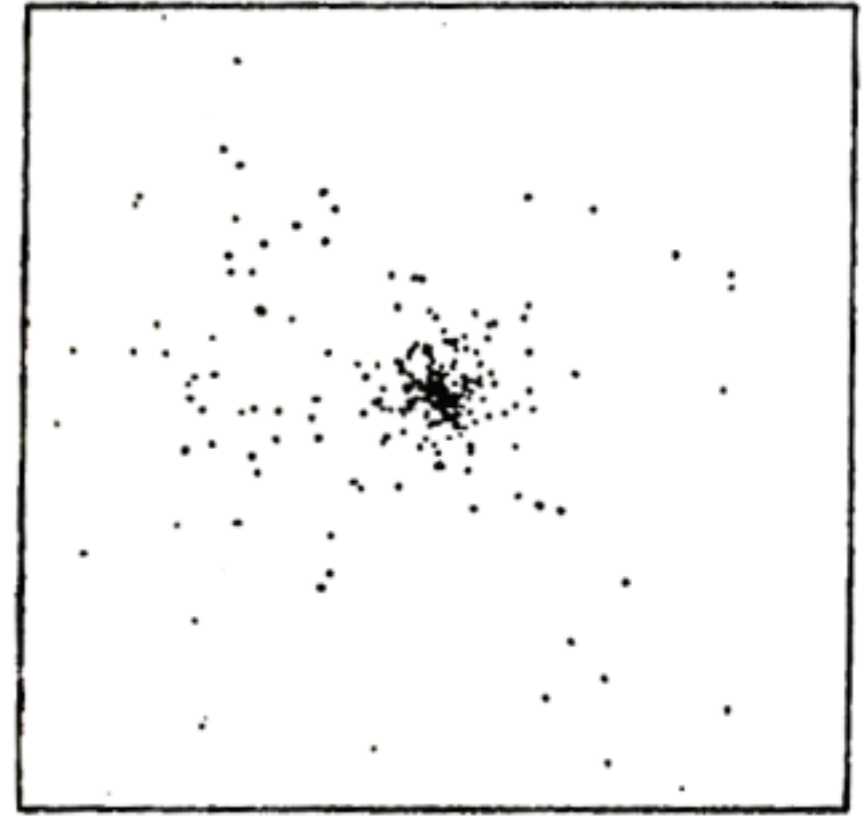
When any region becomes about twice as dense as typical regions its size, it reaches a maximum radius, *stops expanding,*

Simulation of top-hat collapse:
P.J.E. Peebles 1970, ApJ, 75, 13.

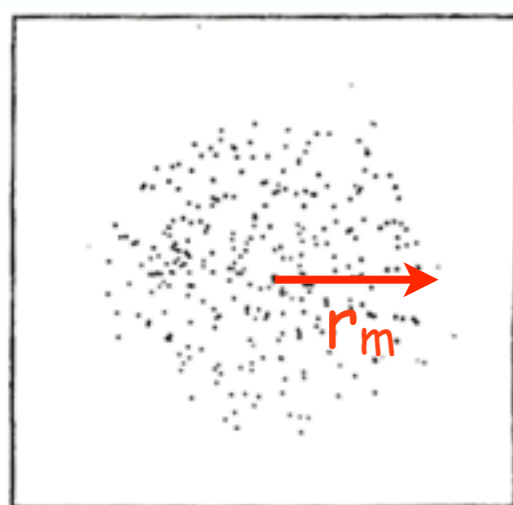


and starts falling together. The forces between the subregions generate velocities which *prevent* the material from *all falling toward the center.*

Used in my 1984 summer school lectures “Dark matter, Galaxies, and Large Scale Structure,” <http://tinyurl.com/3bjknb3>

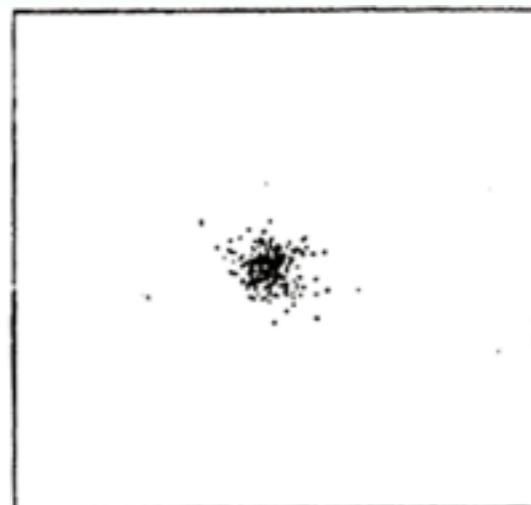


Through Violent Relaxation the dark matter quickly reaches a *stable configuration* that’s about half the maximum radius but denser in the center.

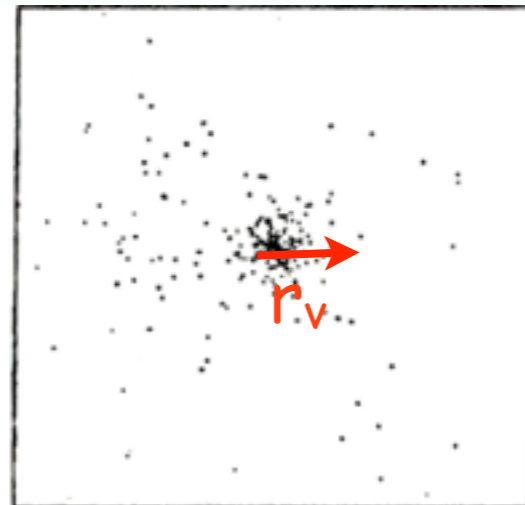


TOP HAT

Max Expansion



VIOLENT
RELAXATION



VIRIALIZED

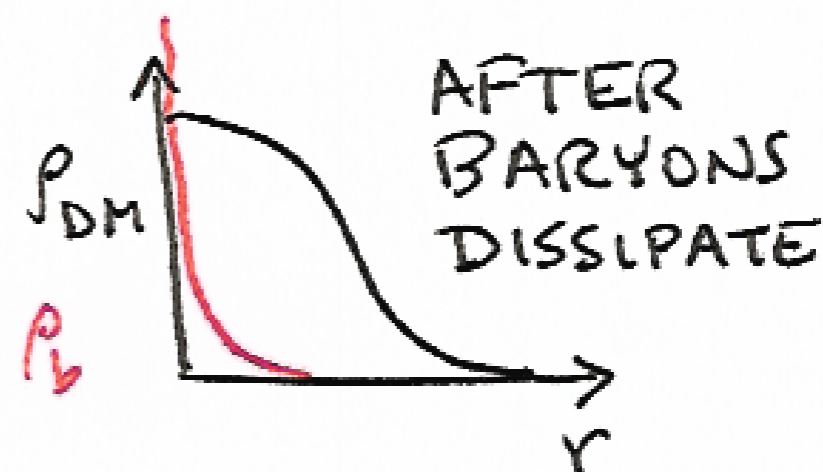
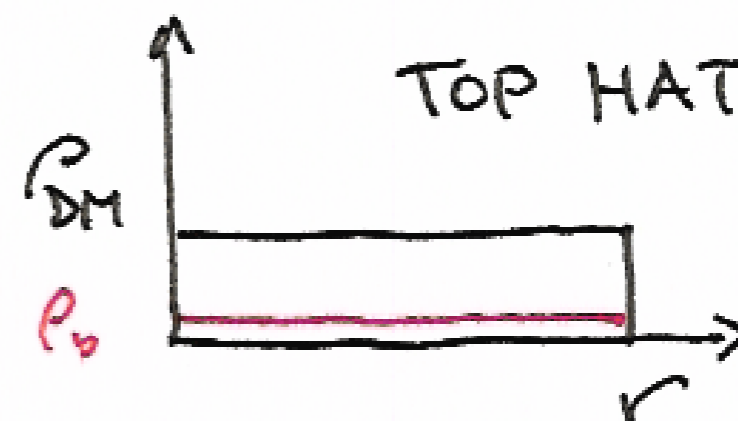
Virial Theorem: $\langle K \rangle = -\frac{1}{2} \langle W \rangle$

$W_m = \frac{C}{r_m}$, so after virialization

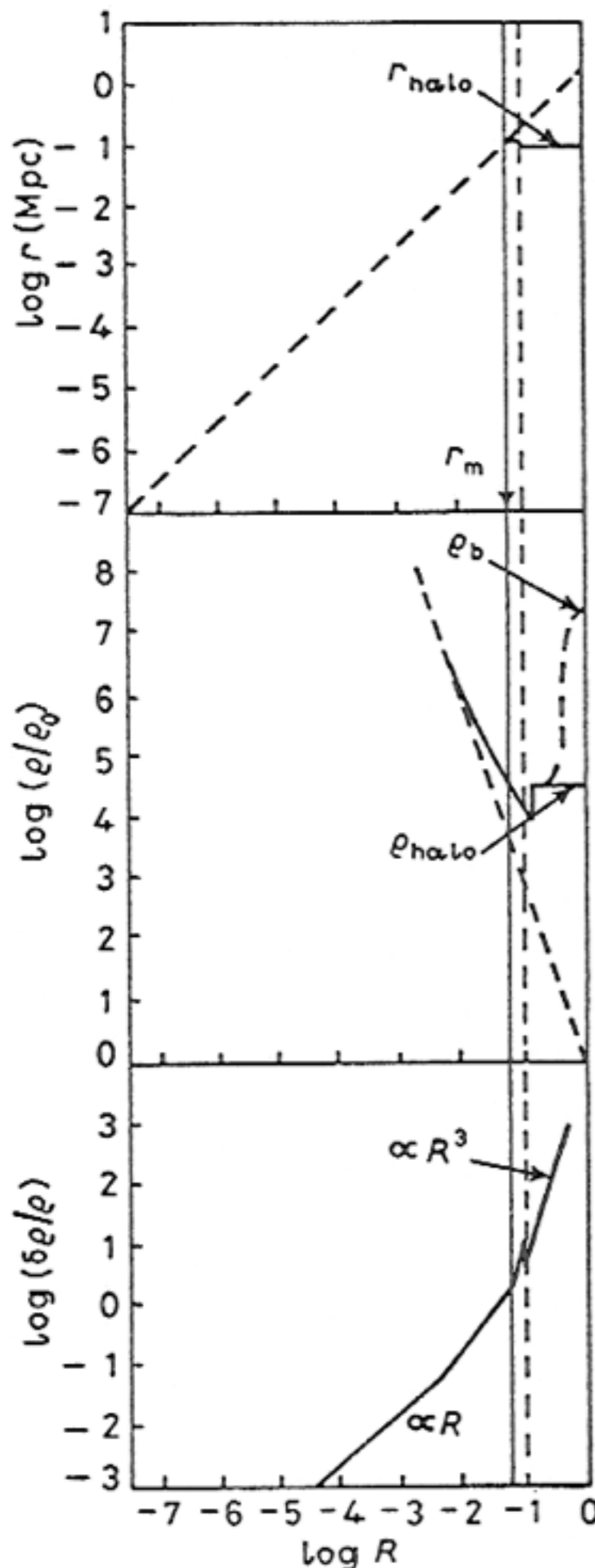
$$\frac{C}{r_m} = E = W + K = \frac{1}{2} \langle W \rangle = \frac{C}{2r_v}$$

$$\Rightarrow r_v = \frac{1}{2} r_m, \quad \rho_v = 8\rho_m \approx 50 \bar{\rho}(t_m)$$

$$\langle v^2 \rangle \approx \frac{GM}{r_v}$$



Growth and Collapse of Fluctuations



Schematic sketches of radius, density, and density contrast of an overdense fluctuation. It initially expands with the Hubble expansion, reaches a maximum radius (solid vertical line), and undergoes violent relaxation during collapse (dashed vertical line), which results in the dissipationless matter forming a stable halo.

Meanwhile the ordinary matter ρ_b continues to dissipate kinetic energy and contract, thereby becoming more tightly bound, until dissipation is halted by star or disk formation, explaining the origin of galactic spheroids and disks.

(This was the simplified discussion of [BFPR84](#); the figure is from my 1984 lectures at the Varenna school. Now we take into account halo growth by accretion, and the usual assumption is that large stellar spheroids form mostly as a result of galaxy mergers [Toomre 1977](#). But now we think that the most intermediate mass stellar spheroids form because of disk instability.)